

# Green Seaweed Starch Nanoparticles: Synthesis, characterization and application

A Dissertation for  
Course code and Course Title: MBT 651- Dissertation  
Credits: 16  
Submitted in partial fulfilment of Master's Degree  
M.Sc. in Marine Biotechnology

by

**MS. MANASI ARUN RANE**

22P0500013  
ABC ID: 921499774924  
PRN: 202207105

Under the supervision of

**DR. MEGHANATH PRABHU**

School of Biological Sciences and Biotechnology  
Biotechnology Discipline



**GOA UNIVERSITY**

**Date: 8<sup>th</sup> April 2024**



Examined by: Sanitahakar  
8/4/24  
*[Handwritten signatures]*

Seal of the School:  
*[Handwritten signatures]*

**DECLARATION BY STUDENT**

I hereby declare that the data presented in this Dissertation report entitled, "**Green Seaweed Starch Nanoparticles: Synthesis, characterization and application**" is based on the results of investigations carried out by me in the School of Biological Sciences and Biotechnology at Goa University under the Supervision of **Dr. Meghanath Prabhu** and the same has not been submitted elsewhere for the award of a degree or diploma by me. Further, I understand that Goa University or its authorities will be not be responsible for the correctness of observations / experimental or other findings given the dissertation.

I hereby authorize the University authorities to upload this dissertation on the dissertation repository or anywhere else as the UGC regulations demand and make it available to any one as needed.



Ms. Manasi Rane

22P0500013

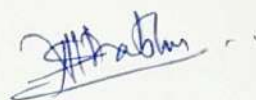
M.Sc. Marine Biotechnology

Date: 8<sup>th</sup> April 2024

Place: Goa University

**COMPLETION CERTIFICATE**

This is to certify that the work entitled, "**Green Seaweed Starch Nanoparticles: Synthesis, characterization and application**" is a bonafide work carried out by **Ms. Manasi Rane** under my supervision in partial fulfilment of the requirements for the award of the degree of Master of Science in Marine Biotechnology at the School of Biological Sciences and Biotechnology, Goa University.



Dr. Meghanath Prabhu

Assistant Professor

Discipline of Marine Biotechnology

Date: 8/4/24



Prof. Bernard F. Rodrigues

Sr. Professor and Dean

School of Biological Sciences and Biotechnology

Date: 8/4/24

Place: Goa University

**Dean of School of Biological Sciences  
& Biotechnology  
Goa University, Goa-403206**



**CONTENTS:**

<b>Chapter</b>	<b>Particulars</b>	<b>Page number</b>
	Preface	v
	Acknowledge	vi
	Tables and Figures	viii
	Abbreviations used	x
	Abstract	xi
1.	Introduction	
	1.1 Background	1-3
	1.2 Aim and Objectives	4
	1.3 Hypothesis/ Research questions	4
	1.4 Scope	5
2.	Literature Review	6-14
3.	Methodology	15-16
4.	Analysis and Conclusions	28-48
	References	49-58
	Appendix	59

## **PREFACE**

In response to the increasing global concern over the environmental impact of synthetic dye contamination in wastewater, this project aims to explore innovative approaches for dye removal and remediation. Building upon the backdrop of the extensive production and discharge of dye-laden wastewater, this study focuses into the potential of starch as a versatile adsorbent for water treatment applications. Specifically, the focus is on harnessing the untapped potential of starch derived from marine seaweed, particularly *Ulva* sp., for dye adsorption.

To date, there has been no reported synthesis of nanoparticles derived from starch extracted from green seaweed *Ulva* sp. This study seeks to pioneer the synthesis of starch nanoparticles sourced from the green seaweed *Ulva* sp. and evaluate their capacity to remove dyes from wastewater. The primary objective of this investigation is to address the treatment of synthetic and hazardous dyes found in wastewater, which are commonly discharged in significant volumes by industries such as textiles, pharmaceuticals, and cosmetics. Through my research, I aim to contribute to the development of effective solutions for mitigating the environmental impact of dye pollution on a large scale.

## **ACKNOWLEDGEMENT**

I extend my sincere gratitude to the Department of Biotechnology (DBT) for their generous support in funding my M.Sc. dissertation.

I extend my sincere appreciation to Prof. B.F. Rodrigues, Dean of the School of Biological Sciences and Biotechnology, Goa University, as well as Prof. Krishnan, Vice-Dean (Research) of SBSB, and Prof. Sanjeev Ghadi, Vice-Dean (Academics) and Programme Director of M.Sc. Marine Biotechnology, for their unwavering support and provision of essential facilities for my research endeavours.

Special thanks to my guide, Dr. Meghanath Prabhu, for his invaluable guidance, assistance, and encouragement throughout my dissertation journey. I am also grateful to the esteemed faculty members of the Discipline of Biotechnology, including Prof. Savita Kerkar, Dr. Sanika Samant, Dr. Samantha Fernandes, Ms. Dviti Volvoikar, Ms. Snesha Bhomkar, and Ms. Snigdha Mayenkar, for imparting their knowledge and expertise during my M.Sc. studies.

I express my heartfelt gratitude to Dr. Sunder Dhuri and Mr. Prajyot Chari from School of Chemical Sciences, Goa University for their assistance in my dissertation in CHNS and FTIR analysis respectively. I am also thankful to Dr. Nitin Sawant from zoology discipline for allowing me to use spectrophotometer and Mr. Madhusudan from Electronics department for helping me in SEM analysis. I am indebted to fellow research scholars, particularly Ms. Diksha, Ms. Hetika, Ms. Priti, Ms. Veda, and Ms. Devika, for their invaluable contributions to the study.

I am also thankful to the non-teaching staff members, including Mr. Serrao, Mrs. Sanjana, Mr. Sameer, Mr. Ashish, Mr. Parijat, Ms. Sandhya, and Ms. Jaya, for their assistance and

support with the logistical aspects of my project. My deepest appreciation goes to my family for their unwavering support, encouragement, and love. Lastly, I extend my gratitude to my friends Ms. Varisha, Ms. Malavika, Ms. Mariya, Mr. Sairaj and Mr. Sushant for their continuous support and motivation.

### List of Tables

<b>Table No.</b>	<b>Description</b>	<b>Page No.</b>
1	Growth of <i>Ulva</i> biomass per week and specific growth rate	29
2	Chemical composition of harvested <i>Ulva</i> biomass	31
3	Comparison of FTIR graph functional groups peaks: theoretical and observed.	38

### List of Figures

<b>Figure No.</b>	<b>Description</b>	<b>Page No.</b>
1	Chemical structure of Congo red	11
2	Chemical structure of Crystal violet	12
3	Chemical structure of Malachite green	13
4	Sampling sites A: Geographic map of sampling sites, B: Sampling at Vagator beach, C: Sampling at Baga beach, D: sampling at Anjuna beach.	15
5	Photoreactor A: 2L, B: 5L, C: 10L volume photoreactors	17
6	In-vitro seaweed cultivation facility Biotechnology discipline, Goa University	18
7	<i>Ulva</i> starch extraction procedure	24
8	<i>Ulva</i> during growth b: <i>Ulva</i> biomass after harvesting	28
9	<i>Ulva</i> thalli observed under 100X objective lens a: without iodine staining b: with iodine staining	32
10	a: Rice starch granule, b: <i>Ulva</i> starch granule	33
11	Graphical representation of concentration of starch samples	33

12	SEM images of a: Rice starch, b: rice starch nanoparticles, c: <i>Ulva</i> starch, d: <i>Ulva</i> starch nanoparticles	35
13	FTIR graph of Rice and <i>Ulva</i> starch	36
14	FTIR graph of Rice and <i>Ulva</i> starch nanoparticles	37
15	Image showing various tubes of Congo red dye (0.1 mg/mL) removal by samples a: control, b: rice starch, c: <i>Ulva</i> starch, d: rice starch nanoparticles, e: <i>Ulva</i> starch nanoparticles, f: dry <i>Ulva</i> biomass	39
16	Image showing graphical representation of percent removal of Congo red dye (Concentration 0.1 mg/mL, 0.5 mg/mL, 1.0 mg/mL) by various samples.	40
17	Image showing various tubes of Crystal violet dye (0.1 mg/mL) removal by samples a: control, b: rice starch, c: <i>Ulva</i> starch, d: rice starch nanoparticles, e: <i>Ulva</i> starch nanoparticles, f: dry <i>Ulva</i> biomass	40
18	Image showing graphical representation of percent removal of Crystal violet dye (Concentration 0.1 mg/mL, 0.5 mg/mL, 1.0 mg/mL) by various samples.	41
19	Image showing various tubes of Malachite green dye (0.1 mg/mL) removal by samples a: control, b: rice starch, c: <i>Ulva</i> starch, d: rice starch nanoparticles, e: <i>Ulva</i> starch nanoparticles, f: dry <i>Ulva</i> biomass	42
20	Image showing graphical representation of percent removal of Malachite green dye (Concentration 0.1 mg/mL, 0.5 mg/mL, 1.0 mg/mL) by various samples.	42
21	Congo red dye concentration A: 0.1mg/mL, B: 0.5mg/mL, C: 1.0mg/mL	44
22	Crystal violet dye concentration A: 0.1 mg/mL, B: 0.5 mg/mL, C: 1.0 mg/mL	45
23	Malachite green dye concentration A: 0.1 mg/mL, B: 0.5 mg/mL, C: 1.0 mg/mL	47
24	Standard graph of total protein estimation in dry <i>Ulva</i> biomass	60
25	Standard graph of total carbohydrate estimation in dry <i>Ulva</i> biomass	60

**Abbreviations**

<b>Sr. No.</b>	<b>Abbreviation</b>	<b>Entity</b>
1.	Fig.	Figure
2.	SEM	Scanning Electron Microscopy
3.	FTIR	Fourier Transfer Infrared Spectrometry
4.	°C	Degree Celsius
5.	%	Percentage
6.	mg	Milligram
7.	mL	Millilitre
8.	µg	Microgram
9.	µL	Microliter
10.	g	Gram

### **Abstract**

This research project investigates the potential of *Ulva* seaweed starch nanoparticles for removal of synthetic dyes from wastewater. This study began with the successful collection of *Ulva* samples from diverse locations, capturing various life stages of the seaweed's cycle. In-vitro cultivation experiments revealed substantial growth and development of *Ulva* biomass, supported by visual observations of healthy thalli exhibiting active photosynthesis and its specific growth rate. Biomass characterization was done by proximate and ultimate analyses, which highlights the rich composition of *Ulva* biomass, with high proportions of carbohydrates, proteins, lipids, and starch. Microscopic analysis confirmed the presence of starch granules within *Ulva* thalli, providing visual evidence of their suitability for further processing. The starch granules were extracted from harvested *Ulva* biomass from in-vitro cultivation and characterised. Further, starch nanoparticles were synthesized from extracted *Ulva* starch. Characterisation of these nanoparticles was done by Scanning Electron Microscopy (SEM) and Fourier Transform Infrared Spectroscopy (FTIR) comparing with conventional terrestrial starches. The results of SEM images revealed that size of *Ulva* starch nanoparticles to be 290 nm and rice starch nanoparticles to be 247 nm. FTIR analysis confirmed the presence of distinct functional group of conventional starch on *Ulva* starch and its nanoparticles. Their potential as functional biomaterials, for treatment of synthetic dyes in wastewater was studied. Dye removal experiments showcased the remarkable efficiency of *Ulva* starch nanoparticles in environmental remediation, underscoring their promise for addressing pollution challenges. Overall, this research project sheds light on the potential of *Ulva* seaweed starch nanoparticles in wastewater treatment and paves the way for further exploration in biotechnology, environmental science, and beyond.

## **CHAPTER 1: INTRODUCTION**

### **1.1 Background**

In the year 2023, around 70 billion tons of wastewater containing synthetic dyes was produced (Lin et al., 2023). These dyes are utilized across diverse sectors such as textiles, food manufacturing, pharmaceuticals, cosmetics and many more. Each year, the global production of textile dyes exceeds 10,000 tons, with approximately 100 tons of dyes being discharged into wastewater on a yearly basis (Semeraro et al., 2015). Unfortunately, roughly 80% of this dye-laden wastewater is either discharged into water bodies such as oceans or rivers without treatment or directly employed for irrigation purposes (Lin et al., 2023). As these dyes are synthetic and non-biodegradable, they remain dissolved in the water bodies.

Dyes possess the ability to absorb light radiation within the visible range, typically from 400 to 700 nanometre. When white light interacts with a surface, undergoes diffusion, or is transmitted through a medium, it transitions from white to coloured light due to selective absorption of energy by specific atoms, known as chromophoric groups. In simpler terms, a dye is a substance that can absorb certain wavelengths of light and then reflect complementary colours (Kumari et al., 2023). This acts as a barrier in sunlight penetration in water which in turn decreases the its aesthetic quality by increasing chemical and biological oxygen demand (Peramune et al., 2022).

Uncontrolled disposal of dye wastewater has severe consequences, posing significant risks to humans, plants, animals and whole natural environment. The harmful effects of dyes present in wastewater can extend to soil, leading to the destruction of microorganisms critical for agricultural productivity. Irrigation with textile industry effluent may result in soil pore blockage and texture hardening, hindering root penetration (Moyo et al., 2022). It is reported that even at low concentrations (1.0 mg/L), the presence of dyes in water renders

it unsuitable for human consumption (Kumar et al., 2018; Velusamy et al., 2021). In a study in India textile wastewater was analysed for concentration of dye, which was found to be 45mg/L (Durairaj and Sivakumar, 2014).

Many new techniques are designed to address this issue. These includes dye removal and dye degradation. Some of the techniques in dye removal are adsorption (Lan et al., 2022), coagulation/flocculation (Al-Tohamy et al., 2022; Afrin et al., 2021), chemical precipitation (Kim et al., 2022), electrochemical oxidation (Kumari et al., 2023), ozonation, membrane filtration (Fang et al., 2017). Various biopolymers such as cellulose with different modifications (Sharma et al., 2024), alginate (Rafiee, 2023), starch (Abd El-Ghany et al., 2023), chitosan and its derivatives (Saiyad et al., 2023), gum with conjugation with nanocomposites and hydrogel (Kumari et al., 2024; Usman et al., 2023).

Starch is the most prevalent biopolymer found in nature, a homopolysaccharide consisting of both linear and branched units derived from variety of sources (Khoo et al., 2023). It is commonly obtained from grains and holds significant importance as a raw material across multiple industries including medicine, food, and chemicals. It has gathered considerable attention in research due to its promising applications in wastewater treatment (Ahamad et al., 2020). Starch is a non-conventional adsorbent. Adsorption of dyes by starch is widely studied wastewater treatment owing to its eco-friendly and non-hazardous nature (Khoo et al., 2023). To increase the dye adsorption potential of starch, various modification on starch and its properties have been carried out such as grafted starch (Ortega-Toro et al., 2016), starch based hydrogels and beads (Ismail et al., 2013), starch nanocomposites and nanoparticles (Abd El-Ghany et al., 2023; Nguyen et al., 2022), starch aerogels (Ganesamoorthy et al., 2021).

However, since starch is one of the important food commodities, using conventional starch for wastewater treatment is not ideal. It is because, worldwide production of starch in 2020 is estimated to range between 88.1 and 97.7 million tons. Among this total, approximately 75 % originates from corn, with cassava accounting for 14 %, wheat for 7 %, and potatoes for 4 % which are all conventional sources of starch (Vilpoux & Santos Silveira Junior, 2023). Thus, usage of conventional sources of starch will only increase the pressure on production demand.

One of the sources of novel starch is marine seaweed. Starch from green seaweed such as *Ulva* sp. is yet to be explored for its full potential (Prabhu et al., 2019). The overlooked potential of seaweed starch can serve as an important substitute for traditional terrestrial starch sources. Seaweed starch shares similar properties and structural characteristics with its terrestrial counterpart. (Prabhu et al., 2019). This research was conducted to investigate the potential of seaweed starch nanoparticles for dye decolorization of wastewater.

## 1.2 Aim and Objectives:

### Aim:

Aim of this study was to investigate the potential of seaweed starch nanoparticles for dye decolorization of wastewater.

### Objectives:

1. Collection, in-vitro cultivation, and characterization of *Ulva* sp. seaweed biomass.
2. Extraction of starch granules from *Ulva* sp. seaweed and its characterization.
3. Production of starch nanoparticles from extracted *Ulva* starch, its characterization
4. Applications of *Ulva* starch nanoparticles in dye remove.

## 1.3 Hypothesis

As *Ulva* sp. seaweed starch is converted into nanoparticles, its surface area increases significantly, enhancing its adsorption/absorption capacity for chemical dyes in industrial wastewater. We hypothesize that *Ulva* starch nanoparticles will effectively remove wide range of chemical dyes from industrial wastewater, leading to the efficient removal of pollutants from wastewater leading to effective treatment of wastewater.

#### 1.4. Scope

*Ulva* seaweed, abundant in marine environments, represents an underutilized resource with potential applications in various industries. Extracting starch from *Ulva* and synthesizing nanoparticles presents an opportunity to valorize this renewable biomass and contribute to sustainable resource management practices. The synthesis of *Ulva* starch nanoparticles allows for the exploration of their adsorption or absorption capabilities to develop efficient solutions for wastewater treatment. Discovering novel adsorbents or absorbent derived from natural sources like *Ulva* seaweed opens possibilities for developing cost-effective and eco-friendly solutions to tackle water pollution challenges.

If *Ulva* starch nanoparticles demonstrate superior adsorption efficiency as hypothesized, they could be integrated into wastewater treatment systems for the removal of chemical dyes, contributing to cleaner effluent discharge. The outcomes of this study can also serve as a basis for further research and development initiatives in the field of environmental nanotechnology. Continued exploration of natural biomaterials like *Ulva* seaweed for nanoparticle synthesis and wastewater remediation could lead to the development of innovative technologies with broader applications in environmental sustainability.

## **CHAPTER 2: LITERATURE REVIEW**

Starch is an odourless, tasteless, soft, white polysaccharide that is insoluble in cold water or alcohol. It serves as a primary storage polysaccharide in plants which can be found in tubers, roots, and seeds of plant kingdom. Starch, the second most abundant polysaccharide on earth, is a natural, cheap, renewable, and biodegradable polymer. Irrespective of the botanical source, starch is a polymer of the six-carbon sugar D-glucose, often referred to as its “building block”. It is a non-reducing sugar with a skeleton made up of two types of molecules: amylose and amylopectin. Amylose is a linear polysaccharide of glucose units linked by  $\alpha$ -1,4-glycosidic bonds, while amylopectin is a branched polymer with both  $\alpha$ -1,4 and  $\alpha$ -1,6-glycosidic bonds. The ratio of these two core components varies according to the source of starch. The varying ratio of amylose and amylopectin in a particular starch renders its unique structure being crystalline, amorphous, or semi-crystalline (Martha et al., 2023). Starch has its unique properties like gelatinization, retrogradation, and swelling power which eventually makes it possible to be utilized in various industries. Starch granules when heated with water at about 52 °C, undergo swelling by absorbing water. Heat disrupts the highly organized and tightly packed granular structure of starch, releasing amylose and amylopectin, which can interact with water and give a paste-like texture or viscous nature. This property of starch is known as gelatinization. Water acts as a plasticizer penetrating the starch which eventually increases randomness in the granule. This process is often exploited in the food industry (Gani et al., 2021). When the gelatinized starch is cooled the amylose starts reassociating itself and forms a more organized structure. This property of starch is called retrogradation. Starch retrogradation is of great interest in food technologies and industries as it profoundly affects the quality, acceptability, and shelf life of starch-based foods. The most common application of starch is for thickening and gelling agents.

There are numerous known sources of starch to date including; cereals and grains, tubers and root vegetables, legumes, fruits, seeds, nuts, rhizomes, etc.

The ocean covers 71 % of the Earth's surface and holds 97% of the planet's water, making it an immense natural resource for humanity (National Geographic Society et al., 2021). Notably, India owns a coastline spanning 7516.6 km, presenting a substantial opportunity to harness the wealth of ocean resources (PMF IAS et al., 2023). Making the most of coastal areas by using them sustainably for farming, like aquaculture and marine agriculture is crucial. If we explore the resources in the ocean responsibly, we could meet the needs of the growing world population and take care of the environment at the same time.

Macroalgae popularly known as seaweeds are diversely present in the littoral and sub-littoral zones of the ocean. Marine seaweeds are classified into three categories according to their pigmentation types; Phaeophyta (brown algae), Rhodophyta (red algae), and Chlorophyta (green algae) (Yang et al., 2021). They have a rich reservoir of various bioactive compounds like polyphenols, amino acids, fatty acids, and dietary fibres, as well as polysaccharides, pigments, and other active compounds. Various industries like pharmaceutical, cosmetics, food, and medicine have been exploiting these compounds for ages owing to their versatile role as anti-inflammatory agents, immunostimulants and immunoregulators, antioxidant activity, and other biological processes (Xu et al., 2023).

Green seaweed being most abundant among macroalgae holds significant importance in marine bioresources. Belonging to the Plantae Kingdom, they harness the sunlight to produce food through the process of photosynthesis like any other terrestrial plant. Similar to terrestrial plants they store starch in chloroplast. The ability of green seaweeds to store starch makes them appealing candidates for sustainable starch production in the context of marine biorefinery processes (Zollmann et al., 2019). It has also been reported that

Rhodophyta possesses distinctive Floridean starch which differs from terrestrial sources of starch due to the absence of amylose (Yu et al., 2002). It is found that the Floridean starch by red algae is stored in the cytoplasm rather than chloroplast which is a characteristic property of red algae (Cian et al., 2015).

### **Starch nanoparticles:**

Broadly, the techniques for creating starch nanoparticles (SNPs) can be categorized as either 'top-down' or 'bottom-up' methods (Martha et al., 2023). In nanotechnology both these strategies involve transforming the larger material to a smaller structure where at least it's one of the dimensions is less than 100 nm size. The top-down method involves breaking the material to nano-size by various chemical, enzymatic, physical, or mechanical means such as ultrasonication, homogenization, gamma radiation, and acid hydrolysis (Martha et al., 2023). Whereas the bottom-up approach describes the process of constructing nanostructures from the bottom, involving the precise arrangement and integration of atoms or molecules through physical and chemical means within the nanoscale range of 1 nm to 100 nm. This method particularly works on controlled manipulation which results in the self-assembly of atoms and molecules (Bayda et al., 2019). The bottom-up methods for starch nanoparticle (SNP) synthesis include nanoprecipitation or self-assembly of starch. Till now most prevalent approach has been top-down due to its ease of nanoparticle preparation but still bears the disadvantage of inefficient synthesis of targeted size and shape of nanoparticles. Whereas, the bottom-up approach has the ability to produce nanoparticles with desirable size and shape with high yield and specificity. However, it still requires advanced instruments and precise chemicals (Abid et al., 2022).

Recently starch nanoparticles are in study for removal of dye by adsorption mechanism. In this Basic blue and Basic yellow dyes were tested against cationic starch nanoparticle (Lawchoochaisakul et al., 2021).

One of the methods of starch nanoparticle synthesis combines vacuum cold plasma and ultrasonication, utilizing corn and potato as source materials. It produces particles with sizes ranging from 300 to 600 nm in square and spherical shapes, with carboxyl as the functional group (Chang et al., 2019). Another method employs ultrasound and nanoprecipitation with DMSO and acetone, using corn, potato, and TKP as sources. The resultant nanoparticles are of spherical shape with urea adsorption properties and hydroxyl functional groups (Pan et al., 2022). The third method involves nano-precipitation, alkali freeze, crosslinking, and H<sub>2</sub>SO<sub>4</sub> hydrolysis using broken rice as the source, generating particles of various sizes with oval and irregular shapes. These nanoparticles exhibit secondary amide and H-bonded hydroxyl groups (Chutia et al., 2021).

A fourth approach employs ball-milling and acid hydrolysis with waxy maize as the source, producing irregularly shaped nanoparticles ranging from 60 to 300 nm (Xiao et al., 2020). Another method combines enzymolysis with pullulanase and nano-precipitation using ultrasound. The source used is *Cyperus esculentus*, resulting in spherical nanoparticles with sizes ranging from 190 to 270 nm, having properties like biocompatibility and biodegradability with ether and carboxyl functional groups (Dia et al., 2018).

One of the green synthesis methods employs enzymolysis and recrystallization with maize as the source of starch which yields irregularly shaped nanoparticles ranging from 60 to 120 nm. These nanoparticles exhibit anhydroglucose rings and inter- and intra-molecular hydroxyl groups, finding application in the biomedical field (Yan et al., 2022). Ultrasonication is used for cornstarch nanoparticles, resulting in platelet-shaped, 40 and 60 nm sized nanoparticles with amorphous structure. Serving as a Pickering stabilizer, these nanoparticles hold potential in various applications. Another popular approach utilizes high-pressure homogenization with corn, producing spherical nanoparticles in the range of 10-20 nm with hydroxyl functional groups (Boufi et al., 2018).

Maize is also utilized in a different high-pressure homogenization method, yielding pie-shaped nanoparticles with a rough surface. The nanoparticles are of size 200 nm with the hydroxyl functional group (Gou et al., 2019; Liu et al., 2009). A one more distinct method involves dry heating and mild acid treatment of maize, resulting in spherical nanoparticles of less than 100 nm for industrial applications (Wei et al., 2018).

The last method employs alpha-amylase with maize, potato, and cassava as sources, producing octahedral nanoparticles of less than 400 nm. These nanoparticles exhibit strong hydrogen bonds and biodegradability, finding applications in bio-composites and pharmaceuticals (Kim et al., 2017).

### **Environmental impact of synthetic dyes**

A colorant can be pigments or dyes. Pigments exhibit high insolubility in water, and their constituent particles typically vary in size from 1 to 2 micrometres. In contrast, dyes readily dissolve in water and typically possess particle sizes ranging from 0.025 to 1.0 micrometres (Braun, 1983). A dye is a compound employed to add colour to textiles, paper, leather, and various materials, ensuring that the colour remains stable and resistant to alteration from washing, heat, light, or other environmental factors that the material may encounter (Abrahart, 1977).

Dyes find applications across a wide array of industries including textiles, paper production, food colouring, printing, leather tanning, artistic endeavours, and plastics manufacturing. Moreover, they serve as colouring agents in pharmaceuticals, are utilized for staining biological specimens, and have medical applications in human treatment (Teo et al., 2022). Dyes are often labelled as recalcitrant pollutants due to their intricate aromatic structure characterized by delocalized electrons and conjugated double bonds. These features render them chemically stable, greatly soluble in water, resistant to biodegradation, and capable of

persisting in the environment for prolonged durations which makes them an ideal for industrial application (Al-Tohamy et al., 2022).

The persistent nature of dyes in aerobic environments, particularly within traditional treatment facilities, contributes to their accumulation in sediments, soil, and eventual transport into public water systems (Vikrant et al., 2018). While many dyes exhibit resistance to environmental degradation, some may undergo partial degradation or transformation in anoxic conditions, such as the reduction of azo-type compounds leading to the formation of potentially hazardous aromatic amines. Additionally, there is a risk of dyes reacting with intermediate synthetic compounds or their degradation byproducts, potentially generating mutagenic and carcinogenic substances (Lellis et al., 2019). For the study three such dyes are utilized; Congo red, crystal violet, and malachite green.

### Congo red

Congo red (CR), also known as 1-naphthalene sulfonic acid, 3,3'-(4,4'-biphenylenebis(azo))bis(4-amino-)disodium salt, is classified as a benzidine-based anionic diazo dye (Zeng et al., 2014) (**Fig 1**).

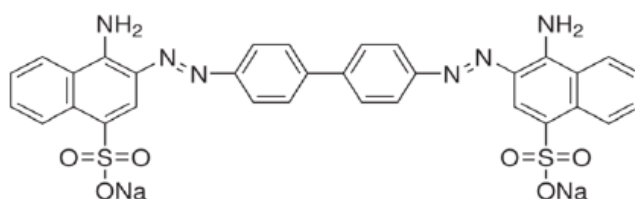


**Fig. 1:** Chemical structure of Congo red (Khan et al., 2020).

It is expected to undergo metabolism, potentially converting into benzidine, a substance known to be carcinogenic to humans. CR exhibits a complex chemical structure, high

solubility in water, and considerable persistence in the environment following discharge (Chatterjee et al., 2010). Despite being recognized as a human carcinogen and being banned in numerous countries due to associated health risks; CR continues to be widely utilized in various regions (Afkhani & Moosavi, 2010). Following the reduction of azo dyes, mutagenic activity has been observed. The aromatic amines generated as metabolites during this reduction process can exhibit toxic effects based on their chemical structure in comparison to the original compound. Additionally, the reduction of azo dyes has the potential to produce DNA adducts, which may pose toxicity risks even to microorganisms involved in the discoloration process (Alderete et al., 2021).

### Crystal violet

Crystal Violet (CV), also referred to as gentian violet in its impure form, is a type of triphenylmethane dye that has found widespread applications in both human and veterinary medicine. It is commonly utilized as a biological stain in medical laboratories and clinics, as well as in the textile processing industry for dyeing fabrics. Crystal Violet is classified as a cationic dye, characterized by the presence of one dimethylamino group on each phenyl ring. (Fig. 2).

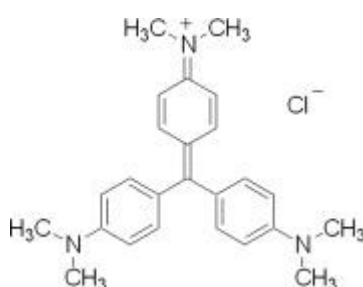


**Fig. 2:** Chemical structure of Crystal violet (Mona et al., 2011)

Toxicological studies have shown that CV is highly toxic to mammalian cells and may lead to respiratory and kidney failure in extreme cases. It is also considered a biohazard substance due to its harmful effects. Moreover, CV is readily absorbed by fish and can induce carcinogenic and mutagenic effects in rodents, increasing the risk of human bladder cancer. Studies on the genotoxic effects of CV have revealed its cytogenetic toxicity and potential mutagenic activity (Hashimoto et al., 2013; Mani & Bharagava, 2016). CV has been found to cause DNA damage and induce sister chromatid exchanges. Moreover, chronic exposure to CV has been associated with the development of liver neoplasms in mice, highlighting its carcinogenic potential. CV is a cytogenic, genetic, mutagenic and carcinogenic agent causing severe health hazards in human such as skin irritation, digestive tract irritation, respiratory and kidney failure, etc (Xiao et al., 2020).

### Malachite green

Malachite green (MG) is categorized as a water-soluble basic dye and falls under the diamino derivative in the triphenylmethane class of dyes (**Fig 3**).

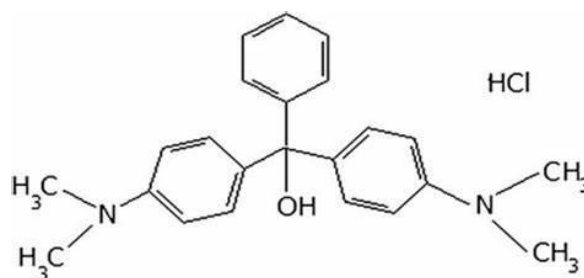


**Fig. 3:** Chemical structure of Malachite green (Chinenye Adaobi Igwegbe, 2014)

It presents as a crystalline green-coloured powder, drawing its name from its resemblance to the mineral malachite's colour (J. Sharma et al., 2023). Malachite green dye (MGD) finds extensive application as a cationic dye in industries such as textiles, paper, and leather

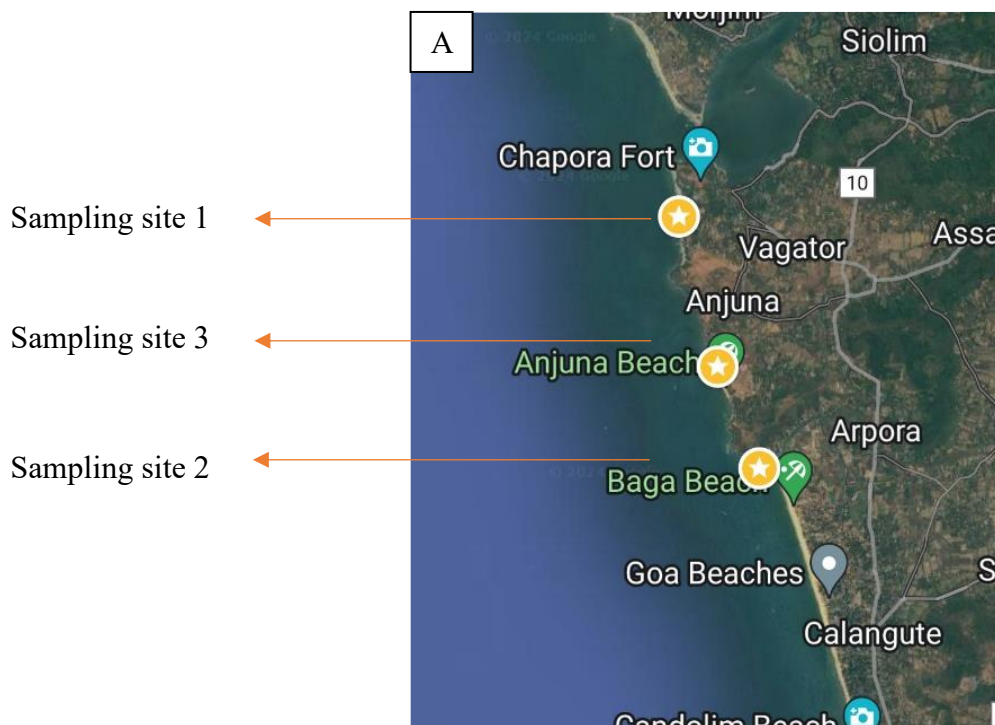
(Verma et al., 2020). While it serves as an antiseptic and therapeutic agent for treating fish diseases caused by fungi, bacteria, and parasites, MGD poses significant hazards, regardless of its external uses. Suspected of causing various ailments including carcinogenicity, mutational instability, and pulmonary toxicity, MGD's high toxicity and low biodegradability pose challenges for traditional removal methods from aqueous solutions (Xiao et al., 2020). Consequently, new technologies such as adsorption, membrane filtration, ion exchange, chemical oxidation, aerogel, and photocatalytic degradation have garnered significant attention (Verma et al., 2020).

## CHAPTER 3: METHODOLOGY

### 3.1 Sample collection and cultivation

#### 3.1.1 Seaweed sample collection

Specimens of green seaweed *Ulva* sp. were collected from three different locations in Goa, India. Samples were collected from intertidal zone at low tide. Sampling dates and time were selected using online tide timetable ([tide-forecast.com](http://tide-forecast.com)). The initial collection occurred on October 28<sup>th</sup>, 2023, at Vagator beach, Goa-403509, India (latitude: 15.59993°, longitude: 73.734145°). The second sampling site was Baga beach, Goa-403509, India (latitude: 15.561747°, longitude: 73.746295°), on November 27<sup>th</sup>, 2023. The third sampling was conducted on December 19<sup>th</sup>, 2023, at Anjuna beach, Goa-403509, India (latitude: 15.577206°, longitude: 73.739685°). Despite being three different locations, all three sampling sites were located on same stretch of the Goa's coastline (**Fig.4**).



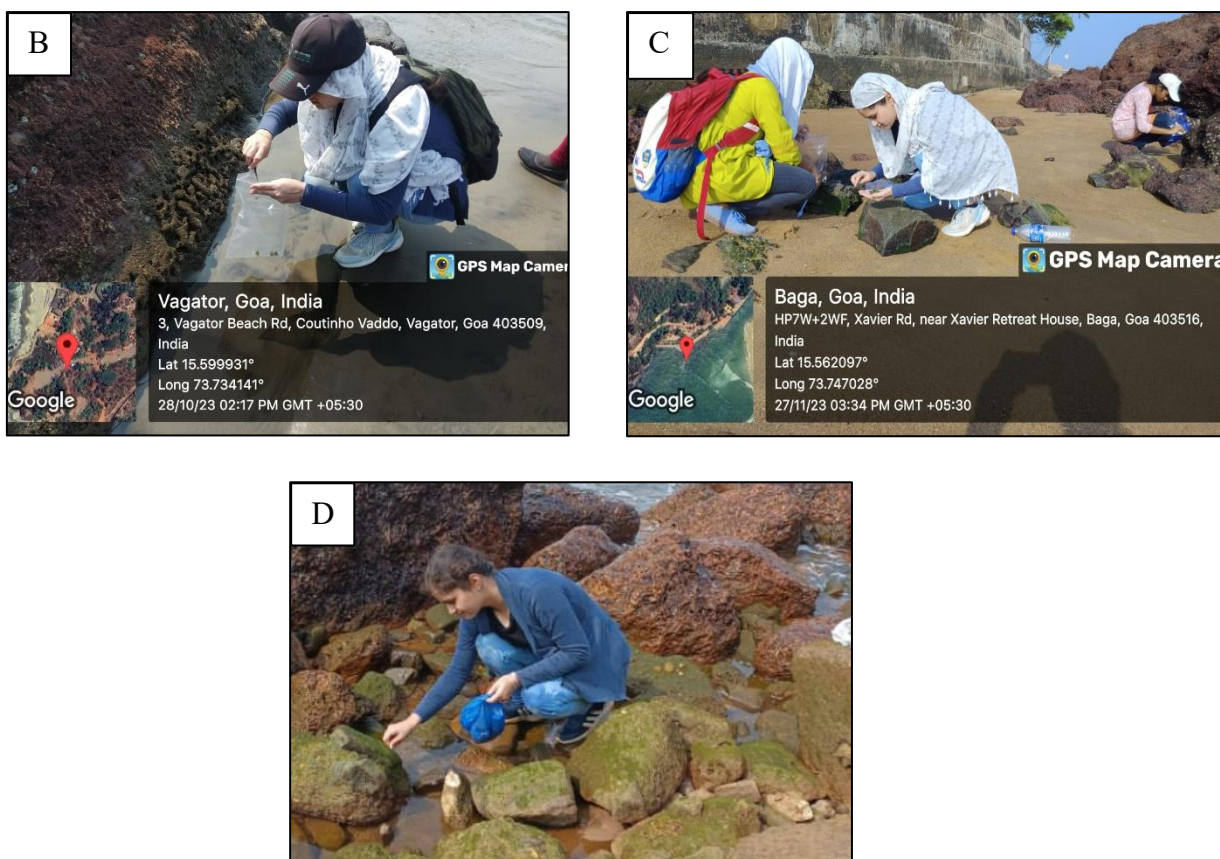


**Fig. 4:** Sampling sites **A:** Geographic map of sampling sites, **B:** Sampling at Vagator beach, **C:** Sampling at Baga beach, **D:** sampling at Anjuna beach.

Samples were brought back to laboratory and were undergone further processing.

### 3.1.2 In-vitro seaweed cultivation

Collected seaweed specimens were meticulously cleaned to eliminate any associated marine organisms and sand particles using forceps and multiple rinses with seawater sourced from the same sampling site. For cultivation purpose seawater was filtered with muslin cloth and subsequent sterilization via autoclaving at 121°C and 15 psi, for 20 minutes. Cleaned seaweed samples was seeded for cultivation in photoreactors of capacity 2, 5, and 10 liter (**Fig. 5**).

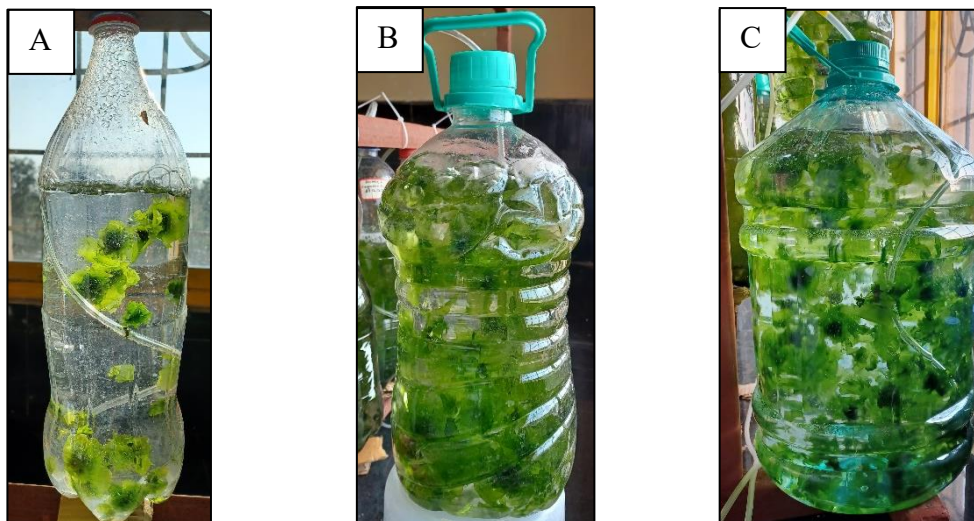


**Fig. 5:** Photoreactor A: 2L, B: 5L, C: 10L volume photoreactors

Salinity was adjusted at 25 PSU using distilled water and measured by using Refractometer (Erma Head Refractometer). Seeding density was initially maintained as 2.5 g/L. The nutrients supplied were monosodium phosphate ( $\text{NaH}_2\text{PO}_4$ ) and ammonium chloride ( $\text{NH}_4\text{Cl}$ ) at the concentration of 0.057 mM/L and 0.59 mM/L respectively. Here,  $\text{NaH}_2\text{PO}_4$  and  $\text{NH}_4\text{Cl}$  were used for providing as source of phosphorous and nitrogen respectively.

Throughout the cultivation period, seawater in the culture vessels underwent weekly replacement, while nutrients were replenished every alternate day. Temperature was maintained at  $24 \pm 2$  °C, with continuous aeration provided. Additionally, tube lights were employed as supplementary light sources during daylight hours. Light intensity was measured using Lux meter at 10 am, 1 pm, 6 pm which was found to be 1429.33 lux, 5300.33 lux, 28842.66 lux respectively.

The seaweed samples were cultivated for duration of four weeks maintaining all culture conditions. After every week the biomass was weighed for analysing growth.

The cultivation setup was situated in Seaweed cultivation facility at Biotechnology laboratory, School of Biological Sciences and Biotechnology (SBSB) of Goa University (Fig. 6).



**Fig. 6:** In-vitro seaweed cultivation facility Biotechnology discipline, Goa University

Specific growth rate in percentage per day was calculated by using formula (Yong et al., 2013):

$$\text{Specific growth rate (g day}^{-1}\text{)} = \left[ \left( \frac{W_t}{W_o} \right)^{1/t} - 1 \right] \times 100$$

Where,  $W_t$  is Final weight,  $W_o$  is initial weight,  $t$  is time period (7 days)

### 3.2 *Ulva* biomass characterization

The cultivated biomass was harvested after each culture cycle. It was dried overnight at 80 °C and ground using liquid nitrogen in a mortar and pestle till fine powder was formed. For all characterization tests powdered dry biomass was used.

### 3.2.1 Proximate analysis

Estimation of moisture, ash, total solids and volatile solids content:

Ash and moisture in the biomass were determined by following procedure given by (Shadangi et al., 2023). The ash content present in the biomass is nothing but residual inorganic matter left behind after combustion at higher temperature. These inorganic components typically comprise of minerals such as silica, calcium, potassium, iron, sodium, magnesium, aluminum, titanium and others. Presence of these minerals depends on the source of plant material.

To determine the ash content (in %), moisture from the biomass has to be eliminated. Sample (0.2g) dry *Ulva* biomass (W2) was first oven-dried at  $105 \pm 2$  °C overnight in pre-weighed crucible (W1). Weight is noted as W3. For volatile solids oven-dried sample was heated in the muffle furnace (Parthak electronic furnace) at  $550 \pm 25$ °C for three hours, cooled in the desiccator and the final weight is noted as W4.

Formulas: ***Total solids (%) = (W3-W1/W2) \*100***

W1= weight of the crucible (g)

W2 = weight of sample

W3 = Dry weight of sample + crucible (g)

***Ash content (%) = (W4-W1/W2) \*100***

W4 = Weight of crucible + sample after 550°C (g)

***Volatile Solids (%) = 100- Ash content (%)***

***Moisture content (%) = 100 - Total solids (%)***

### 3.2.2 Ultimate analysis

The elemental composition of *Ulva* was determined by CHNS analysis of dry biomass using CHNS analyzer Elementar® Vario Micro Cube analyser V1.9.4. It is an organic elemental analysis or elemental microanalysis which determines the amounts of carbon (C), hydrogen (H), nitrogen (N) and sulphur (S) present in a sample.

### 3.2.3 Chemical composition analysis

#### a. Estimation of total protein content

Folin's Lowry method (Lowry et al., 1951) was used for determination of total protein in dry *Ulva* biomass. Bovine Serum Albumin (BSA) working standards of concentration (0.04, 0.08, 0.12, 0.16, 0.20 mg/mL) were prepared. Fifteen milligram of finely ground *Ulva* biomass was added to 1.5 mL of 0.25 N NaOH in two milliliter tubes and homogenized in bead beater (Benchmark beadbug™ Mini Homogenizer Model D1030 (E)) for 10 minutes and kept in refrigerator overnight. Samples were centrifuged and 1mL from supernatant was taken for protein estimation. Five milliliter Reagent C was added to all test tubes and content was mixed using a vortex. After 10 minutes of incubation at room temperature 1.5 mL Reagent D was added immediately with continuous mixing. Tubes were incubated for 30 minutes at room temperature in the dark. The absorbance of standards and sample was recorded at 660 nm using a Spectrophotometer (UV mini 1240 Shimadzu, Japan). Concentration of protein in *Ulva* sample was estimated from concentration of BSA standard curve plotted against their absorbance.

#### b. Estimation of total carbohydrate content

For estimation of total carbohydrate content Anthrone's test (Ludwig et al., 1956) was employed. From stock solution (concentration 1 mg/mL), working standards were

prepared (0.1 mg/L to 1mg/mL). For sample preparation 10 mg *Ulva* dry biomass was kept in boiling water bath for 3 hours. Five milliliters freshly prepared Anthrone reagent was added in all the tubes and mixed gently. Tubes were incubated in water bath at hundred degrees Celsius for 10 minutes. After incubation it was allowed to cool and absorbance was recorded at 660 nm using a Spectrophotometer. Concentration of carbohydrate in *Ulva* sample was estimated from concentration of glucose standard curve plotted against their absorbance.

**c. Estimation of total lipid content**

Total lipid content in *Ulva* biomass was estimated by Bligh and Dyer method (Bligh & Dyer, 1959). Dry *Ulva* biomass (0.5 g) was taken in the centrifuge tube to which solvent mixture consisting of chloroform and methanol in a 1:2 ratio was added. Following this, the mixture was homogenized for 2 minutes and left to incubate at room temperature for 24 hours. After the incubation period, 4 mL of chloroform was added to each tube and homogenized for one minute. Subsequently, 4 mL of water was added and homogenized again for 1 minute. Immediately after homogenization, the final solution underwent filtration using a Whatman filter paper No. 1. The resulting solution was then transferred into another tube, allowing the layers to separate. The volume of the bottom layer was recorded and subsequently transferred into a pre-weighed petriplate. Following this, the solution in the petriplate was evaporated, and the petriplate was re-weighed. Total lipid content was measured using following formula where, weight of lipid is difference in weight of petriplate before and after lipid extraction.

$$\text{Total lipid} = \frac{\text{Weight of lipid} \times \text{Volume of chloroform}}{\text{Volume of sample}}$$

**d. Total starch content**

10 mg of dry biomass was taken for estimation of total starch content. Megazyme total starch estimation kit was used to determine the starch concentration.

The Total Starch (AA/AMG) Assay Kit (Megazyme K-TSTA-50A / K-TSTA-100A Assay kit) was used to determine the starch content in *Ulva*. Finely ground powder weighing 10 mg for each sample was placed into 2 mL Eppendorf tubes and treated with 0.2 mL of 2M KOH. The tubes were then placed on a shaker at 150 rpm for 30 minutes at 37 °C, with periodic mixing every 10 minutes by vortexing. Following incubation, the tubes were briefly heated in a boiling water bath for 1 minute to fully dissolve the starch in KOH. Subsequently, 0.8 mL of 1.2 M sodium acetate buffer (pH 3.8) was added to the tubes, followed by the addition of 0.01 mL of amylase and 0.01 mL of amyglucosidase (AMG). The tubes were again incubated at 50 °C for 90 minutes, with mixing every 10 minutes. After incubation, the tubes were centrifuged at 3000 rpm for 10 minutes. In separate 2 mL Eppendorf tubes, 0.01 mL of the supernatant was taken, and 0.3 mL of GODPOD reagent was added. The tubes were further incubated at 50 °C for 20 minutes, and the absorbance was measured at 510 nm. Standard glucose solution (100 mg/mL) and a reaction blank were prepared. The concentration of total starch (%) was calculated using the provided formula:

$$\text{Concentration of starch} = \Delta A \times F \times (D/\text{Sample weight}) \times \text{final Volume} \times 0.90$$

Where,  $\Delta A$  represents the absorbance of the sample against the blank, F is the factor to convert absorbance values to mg glucose, D is the dilution factor, and 0.90 is the conversion factor from free glucose to anhydroglucose, as found in starch.

### 3.2.4 Microscopic analysis

*Ulva* fresh biomass thalli was observed under light microscope at 100X magnification. Cell structure and overall thallus architecture was observed. Thalli was stained using Lugol's Iodine solution to observe the starch granules in fresh biomass.

## 3.3 Extraction of starch granules

### 3.3.1 Extraction of starch granules from fresh *Ulva* biomass

Starch granules from *Ulva* was extracted as per (Prabhu et al., 2019). Freshly harvested biomass from the culture was used for starch extraction. It was washed thrice with distilled water to remove surface salts. The biomass was homogenized in distilled water (1:20 (w/v)) to fine particulate suspension using blender at full speed. The homogenate obtained was filtered through filter membrane of pore size 100 µm to remove large particles and cell debris. Filtrate was kept to settle at 4 °C, after 24 hours the top green extract was carefully discarded so that bottom slurry is retained. The slurry was washed with absolute ethanol several times till the green color is removed. The pellet after ethanol washes was resuspended in distilled water and sequentially passed through 10 and then through 5 µm pore size nylon filters. The final filtrate obtained was centrifuged at 9000 rpm, 4 °C for 10 minutes. Final wash of absolute ethanol was given to the pellet and the starch pellet was air dried at 4 °C (Fig. 7).

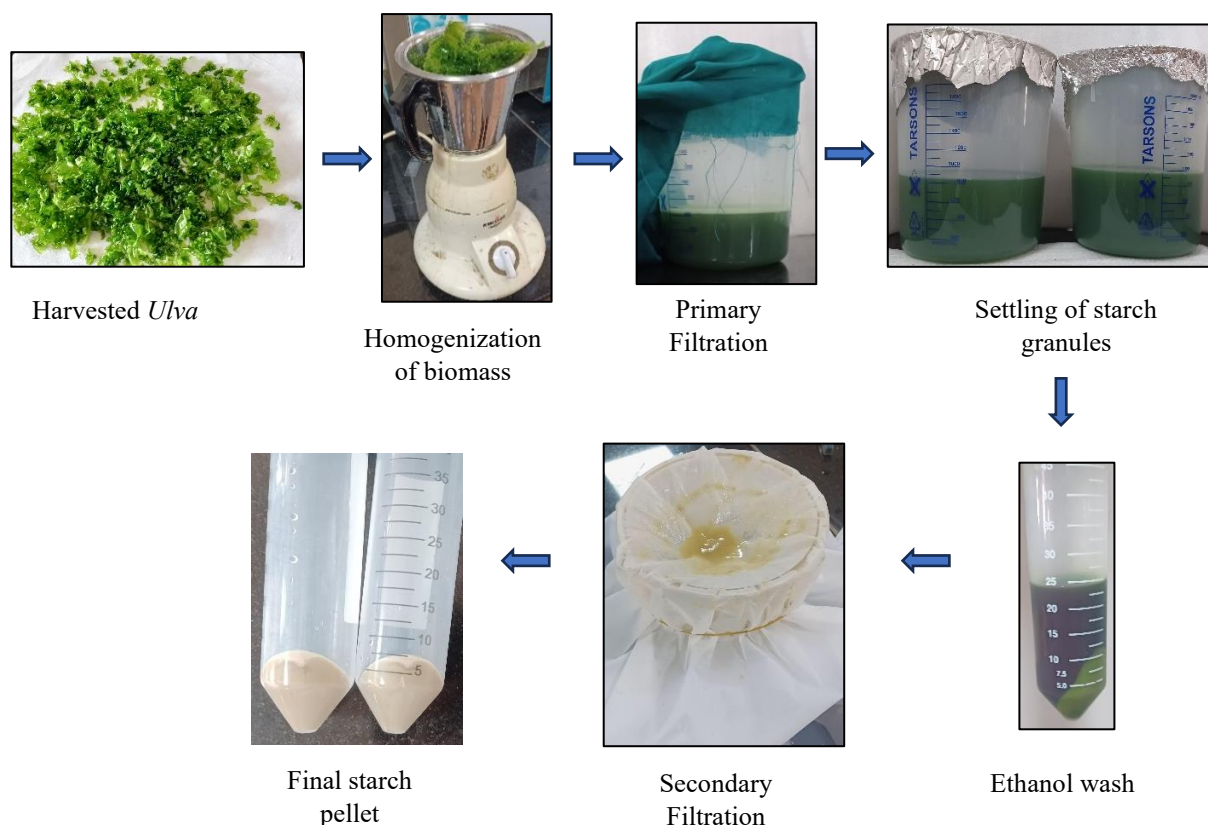


**Fig.7:** *Ulva* starch extraction procedure

### 3.3.2 Extraction of starch granules from rice.

Rice starch was used as a control in all the experiments. Isolation of starch from rice was done according to (Choi et al., 2004).

First rice was steeped in 0.25 % aqueous NaOH solution overnight at room temperature. The steeped sample was blended in blender for 5 minutes at full speed. This step was repeated till a uniform paste was formed. This paste was diluted with distilled water and filtered through 100  $\mu\text{m}$  filter mesh for 3 to 4 times. Filtrate was centrifuged at 25,000 g for 20 minutes followed by ethanol wash of obtained pellet. Top yellowish layer of pellet was removed by scraping followed by ethanol wash to obtain white starch pellet. Pellet was lyophilized to eliminate all moisture content and stored in airtight container.

### 3.4 Synthesis of starch nanoparticles.

Starch nanoparticles were produced through enzymatic hydrolysis according to (Dukare et al., 2021), followed by ultrasonication as described by (Boufi et al., 2018).

For the enzymatic process, 0.15 grams of rice starch and *Ulva* starch were separately suspended in 15 mL of deionized water in two conical flasks. 0.015 units of  $\alpha$ -amylase enzyme, corresponding to a concentration of 0.1 units per gram of starch, was added to each flask. The flasks were then placed in an incubator shaker (Redmi cis-24 plus incubator shaker) set to a temperature of  $60 \pm 0.2$  °C for 30 minutes. Following incubation, the reaction mixtures underwent centrifugation at 9,500 rotations per minute for 10 minutes at 4 °C. The resulting pellet was then resuspended in 15 mL of absolute ethanol.

For sonication (MRC Ultrasonic Processor, SONIC-650WT-V2), above enzymatically treated starch was used with absolute ethanol as a solvent. The sonication parameters were set as: 85 % power output, 220V/50 Hz, 650 W, at 5s pulse and 5s pause for 40 minutes. The tubes were placed in ice bath for reducing the effect of high temperature.

#### 3.4.1. Characterization of starch nanoparticles

For characterization of starch nanoparticles SEM and FTIR analysis techniques were employed.

##### **SEM analysis:**

*Ulva* and rice starch nanoparticles were subjected to scanning electron microscopy (SEM) analysis to characterize their surface structures and particle size. The SEM analysis was conducted using a Carl Zeiss EVO 18 scanning electron microscope. Prior to imaging, the samples were prepared by mounting them onto SEM stubs using double-sided carbon tape and then coated with a thin layer of gold. The SEM images were captured at various

magnifications to investigate the surface topography and particle size distribution of both *Ulva* and rice starch nanoparticles.

### **FTIR analysis:**

Fourier transform infrared spectroscopy (FTIR) was employed to analyze the chemical composition and functional groups present in *Ulva* and rice starch nanoparticles. FTIR spectra were recorded using a Bruker, alpha 2. The FTIR spectra obtained were analysed to identify characteristic absorption peaks corresponding to specific functional groups present in *Ulva* and rice starch nanoparticles, to know their chemical structure and composition.

FTIR spectra were analysed using Origin 8 software (OriginLab Corporation, USA), version v8.0773(773) to identify functional groups and chemical bonds present in the samples. Peak assignments were made based on established literature and spectral libraries.

### **3.5 Dye removal study**

The experiment was carried out by referring to (Cheng et al., 2009) with some modification. Congo red, crystal violet, and malachite green dyes were chosen for the experiment, and solutions with varying concentrations of 0.1, 0.5, and 1 mg/mL were prepared using distilled water for each dye. For each, the maximum absorbance wavelength ( $\lambda_{\max}$ ) was determined. Rice starch (control), *Ulva* starch, rice starch nanoparticles, *Ulva* starch nanoparticles and *Ulva* biomass were taken for analysis. In 2 mL Eppendorf tubes, 10 mg of each sample was added for every 1 mL of dye, and all reactions were performed in duplicate. The mixtures were then incubated under shaking conditions for 15 minutes, followed by centrifugation at 12,000 rpm for 15 minutes.

Absorbance readings were taken at the specific  $\lambda_{\max}$  for each dye using spectrophotometer.

Percent dye removal was calculated by using formula:

$$\% \textit{removal} = \frac{C_o - C_e}{C_o} \times 100$$

Where,  $C_o$ : Initial concentration of dye

$C_e$ : Concentration of dye after the reaction.

### 3.6. Statistical analysis of dye removal by ANOVA

An Analysis of Variance (ANOVA) was conducted using IBM© SPSS version 23.0 statistical software (IBM Corporation, USA, 2021) to examine the percent removal of Congo red, Crystal violet, and Malachite green by various samples, including rice starch, rice starch nanoparticles, *Ulva* starch, *Ulva* starch nanoparticles, and *Ulva* biomass. The provided values for graphical representation of the results represent the mean  $\pm$  standard deviation of two replicates ( $n = 2$ ) for each data point. The significance level was set at  $p < 0.01$ .

Post hoc multiple comparisons using Duncan's test were performed to identify specific differences among the samples. Means marked with different superscript letters indicate statistically significant differences.

## CHAPTER 4: ANALYSIS AND CONCLUSION

### 4.1.1. Sample collection

During first sampling event, both juvenile and mature stages of the seaweed's life cycle were obtained. At second and third location, predominantly juvenile stages of the *Ulva* life cycle were collected. The biomass samples collected at all three locations were obtained during low tide when the intertidal zone was largely exposed, facilitating the collection process. The biomass predominantly adhered to rocks and was carefully removed from the holdfast using forceps before being placed into polyethylene sampling bags.

### 4.1.2. In-vitro seaweed cultivation

The seaweed demonstrated growth and development throughout the experimental period. Visual observation revealed healthy thalli exhibiting characteristic green coloration indicative of active photosynthesis (Fig. 8).

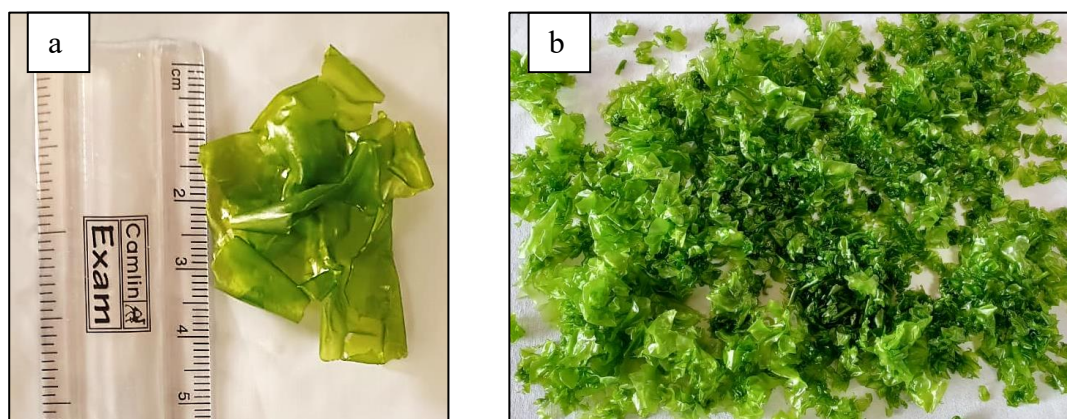


**Fig. 8 a:** *Ulva* during growth, **b:** *Ulva* biomass after harvesting

After analyzing the growth for four weeks, the biomass increased from 7.5 gm on day 0 to 25.12 gm at the end of week four. This biomass increase was 134 % at the end of fourth week. However, the growth rate for first, second, third and fourth week was 7.669 % day<sup>-1</sup>, 4.365 day<sup>-1</sup>, 1.197 day<sup>-1</sup> and 0.865 day<sup>-1</sup> respectively (Table No.1).

**Table No. 1:** Growth of *Ulva* biomass for four weeks and Specific growth rate

Week	Weight (in gram)	Specific growth rate in percentage per day (% day <sup>-1</sup> )
0	7.5	0
1	12.9± 0.14	7.669± 3.79
2	18.59± 0.77	4.365± 2.16
3	21.72± 1.59	1.197± 0.59
4	25.12± 2.71	0.865± 0.42

According to literature the growth rate was  $7.13 \pm 3.44$  % day<sup>-1</sup> with optimum conditions (Balina et al., 2017). This indicate that the biomass increase in initial week is higher than the week later. This could be attributed to the space constraint faced by the *Ulva* biomass during the growth from week 2 to week 4. This suggest that biomass density must be reduced to obtain optimum or maximum growth rate.

One of the primary advantages of in vitro cultivation is the ability to manipulate environmental parameters to optimize growth and productivity. By controlling factors such as light intensity, temperature, nutrient availability, and salinity, researchers can enhance the growth rate and biomass yield of *Ulva* seaweed (Kumar et al., 2023). This allows for the scalable production of biomass for applications ranging from biofuel production to food supplements (Xu et al., 2023).

## 4.2. *Ulva* biomass characterization

### 4.2.1. Proximate analysis

Upon proximate analysis upon dry *Ulva* biomass which was determined by calculating total solids, ash content, volatile solids and moisture content, it was found to be 83.2 % total solids, 18.35 % ash content, 64.80 % volatile solids and 16.73 % moisture content. These

values of ash and moisture content are corresponding to values reported in literature 11.20 % and 16.90 % respectively (Research Center for Oceanography, Indonesian Institute of Sciences, Jl. Pasir Putih No. 1 Ancol Timur, Jakarta 14430, Indonesia & Rasyid, 2017).

The ash content of 10.48 % represents the inorganic mineral content in *Ulva* biomass. It indicates the presence of valuable minerals that can contribute to its potential use as a soil conditioner or in the production of fertilizers (Harris & Marshall, 2017 and Albuquerque et al., 2021).

#### **4.2.2. Ultimate analysis**

It was seen that the carbon content of dry *Ulva* biomass was 25.81 % which closely resembles the carbon content reported in the literature (27.8 % to 30.2 %) (Tsubaki et al., 2020). This suggests that the cultivated *Ulva* biomass may have undergone variations in carbon uptake or assimilation processes, influenced by factors such as nutrient availability, light intensity, and growth conditions (Pappou et al., 2022). Understanding these dynamics is crucial for optimizing biomass production and carbon sequestration potential in *Ulva* cultivation systems.

However, the hydrogen content was 5.57 % which is consistent with literature values (4.7 % to 5.5 %), indicating a relatively stable composition in cultivation conditions. The nitrogen content was observed as 3.22 % which aligns closely with the literature range (3.0 % to 3.9 %), emphasizing the significance of nitrogen as a fundamental nutrient for *Ulva* growth and protein synthesis (Tsubaki et al., 2020). Interestingly, the sulphur content of 4.66 % exceeds the lower limit reported in literature range (2.9 % to 3.9 %) (Tsubaki et al., 2020).

#### 4.2.3. Chemical composition analysis of *Ulva* biomass

The content of total protein in *Ulva* biomass was found to be  $7.67 \pm 0.05\%$  which falls within the range reported in the literature (2-13 %). This indicates that the protein content in the analysed *Ulva* sample is consistent with previous studies. The total carbohydrate content in the *Ulva* biomass was  $50.28 \pm 0.66\%$  which is within the reported literature range (31-80 %). This suggests that the analysed *Ulva* sample is relatively rich in carbohydrates. Carbohydrates are important energy sources and structural components in biomass, indicating the potential of *Ulva* biomass for applications in biofuel production, food, or pharmaceutical industries (Li et al., 2023). The total lipid content measured in the sample was 1.8 %, falling within the literature range (1-3 %). This indicates that the lipid content of *Ulva* is within the expected range based on the literature. The observed content of total starch in *Ulva* biomass was  $3.93 \pm 0.03\%$  which is slightly lower than the literature value (4.2 %). While the difference is relatively small, it highlights the variability in starch content among different *Ulva* samples.

**Table No. 2:** Chemical composition of harvested *Ulva* biomass

Sr. No.	Chemical parameter	Content in dry weight (%)	Values reported in literature (%)	Reference
a	Total Protein	$7.67 \pm 0.05$	2-13	(Pezoa-Conte et al., 2017)
b	Total Carbohydrate	$50.28 \pm 0.66$	31-80	(Kidgell et al., 2019)
c	Total lipids	1.8	1-3	(Putra et al., 2024)
d	Total starch	$3.93 \pm 0.03$	4.2	(Bikker et al., 2016)

However, it's important to note that the biochemical makeup of marine macroalgae can vary considerably depending on factors like species type, growth conditions, and developmental stage. Thus, even when analysing biomass from the same species, variations may arise due

to differences in environmental factors such as salinity, water temperature, depth, and pollution levels (Pappou et al., 2022).

#### 4.2.4. Microscopic analysis

Before staining with iodine, *Ulva* thalli appear green in color, reflecting the presence of chlorophyll, the primary pigment responsible for photosynthesis in algae (Zhao et al., 2023). The thalli exhibit a flat, sheet-like morphology with a smooth texture and a slimy or mucilaginous surface (**Fig. 9a**). After staining with iodine, *Ulva* thalli undergo a noticeable colour change (**Fig. 9b**). The thalli turn dark blue or black, indicating the presence of starch within the cells. Starch, a storage carbohydrate synthesized during photosynthesis, reacts with iodine to form a characteristic blue-black complex, providing a clear indication of starch accumulation in the cells (Prabhu et al., 2019). The stained thalli retain their overall morphology, but the contrast between the cells and the background significantly improves, allowing for better visualization and analysis under a microscope.

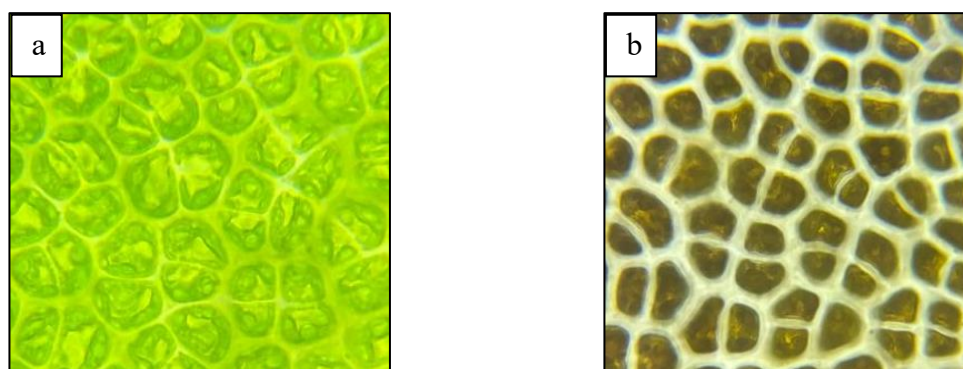


**Fig. 9:** *Ulva* thalli observed under 100X objective lens

**a:** without iodine staining, **b:** with iodine staining

#### 4.3. Extraction of starch from *Ulva* biomass

The successful extraction and microscopic observation of starch granules from *Ulva* seaweed demonstrate the feasibility of utilizing seaweed as a potential source of starch. From

harvested *Ulva* biomass of 121 g, 0.89 g starch was obtained. Its observation under light microscope with iodine staining was done for confirmation starch granules. Under 100X objective lens brown black coloured starch granules were seen in Fig 10a and 10b.

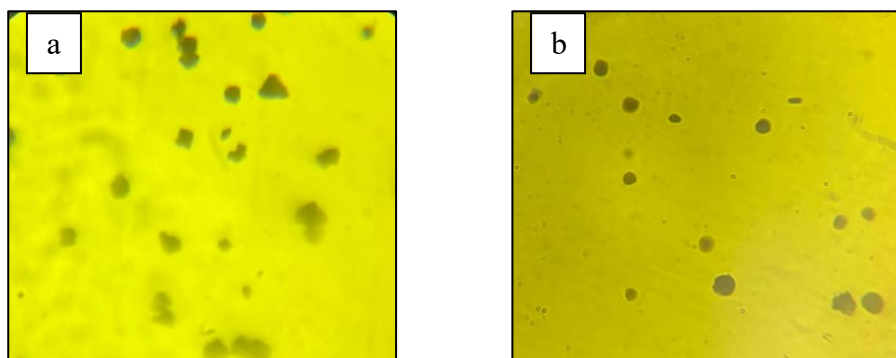


**Fig. 10:** Iodine-stained starch samples

**a:** Rice starch granule, **b:** *Ulva* starch granule

The starch concentration within *Ulva* biomass was notably low, contrasting with the extracted *Ulva* starch, which exhibited a concentration of 82.5 % (**Fig. 11**).

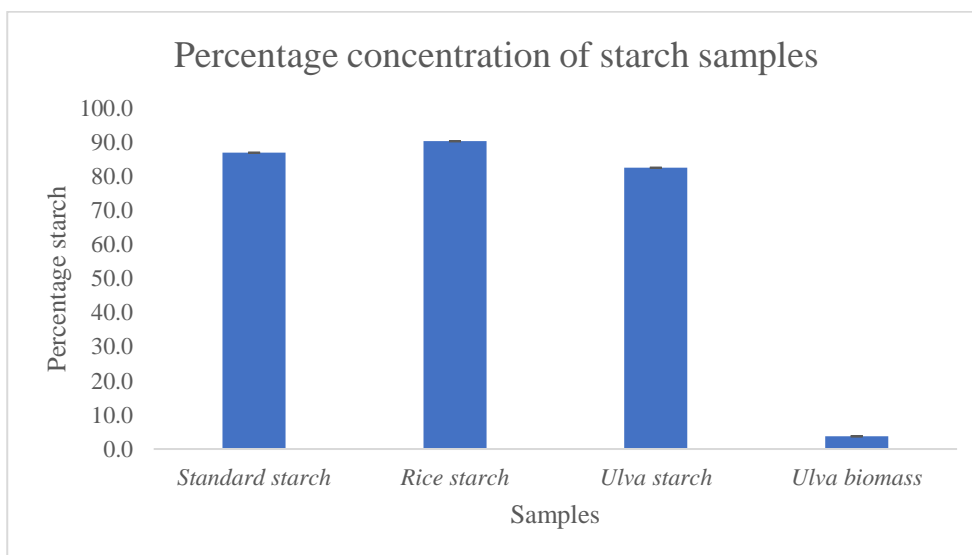


**Fig. 11:** Graphical representation of concentration of starch samples

### 4.3.1 Starch nanoparticles characterization

#### SEM analysis

Scanning electron microscopy provide valuable insights into the structural features of the synthesized starch nanoparticles. The SEM images of synthesized starch nanoparticles revealed their morphological characteristics at the nanoscale level. The spherical morphology suggests a controlled synthesis process, for starch nanoparticle synthesis.

The SEM analysis revealed distinct differences in the morphological characteristics of starch granules derived from rice and *Ulva* seaweed with respective nanoparticles (**Fig. 12**). The average size of rice starch granules was measured to be approximately 5  $\mu\text{m}$ , exhibiting a polyhedral shape (**Fig 12a**), whereas *Ulva* starch granules displayed a smaller average size of around 3  $\mu\text{m}$  and a more spherical morphology (**Fig 12c**). Following enzymatic treatment with  $\alpha$ -amylase for 30 minutes and subsequent ultrasonication for 40 minutes, significant size reduction was observed, with rice starch granules decreasing to an average size of 200 nm (**Fig 12b**) and *Ulva* starch granules reducing to average size 329.6 nm (**Fig 12d**). These findings demonstrate the effectiveness of enzymatic hydrolysis and ultrasonication in reducing the size of starch granules, leading to the formation of nanoparticles suitable for various applications.

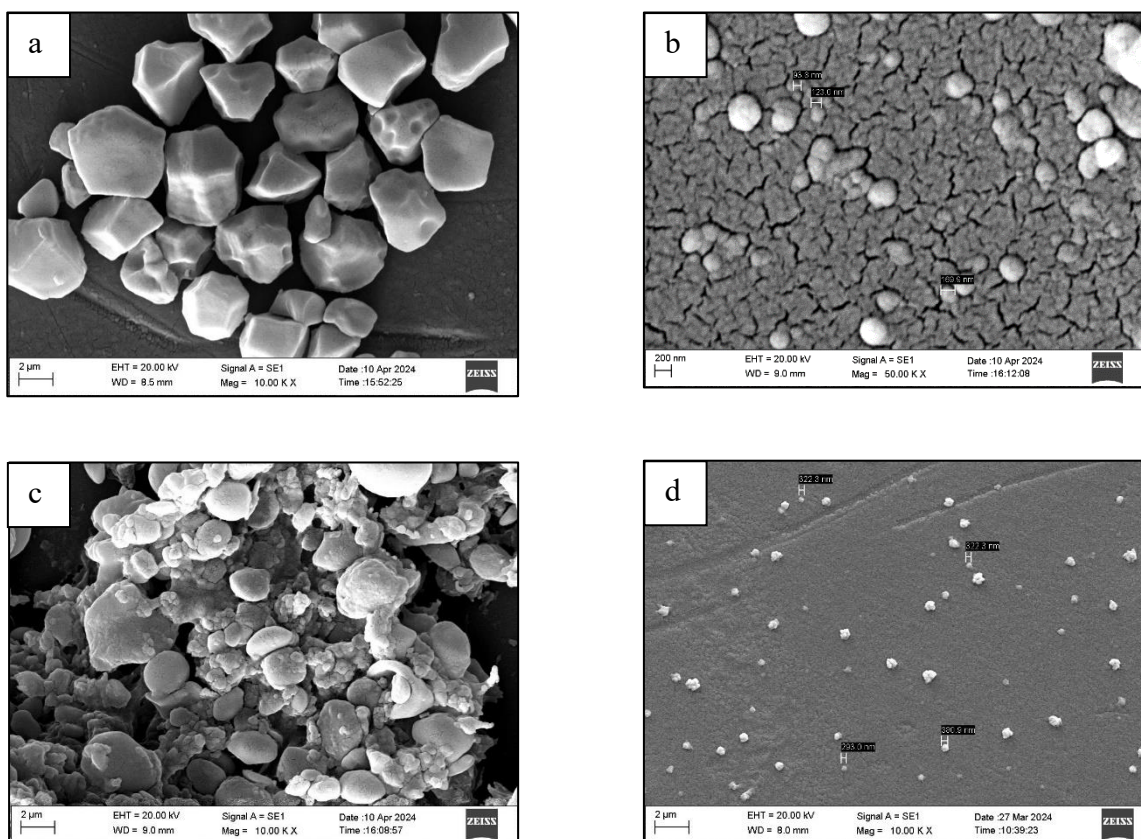


**Fig. 12:** SEM images of **a:** Rice starch, **b:** rice starch nanoparticles, **c:** *Ulva* starch, **d:** *Ulva* starch nanoparticles

### FTIR analysis

In Fourier Transform Infrared Spectroscopy (FTIR) analysis of rice starch *Ulva* starch, various peaks provide valuable information about its molecular structure and functional groups (**Fig 13**). Usually the O-H stretching peak are typically observed in the range of  $3200-3600\text{ cm}^{-1}$ , signifies the presence of hydroxyl groups within the starch molecule. Correspondingly, the C-H stretching peak, appearing around  $2900-2950\text{ cm}^{-1}$ , indicates the stretching vibrations of C-H bonds present in alkyl groups of the starch molecule. Another peak is the C=O stretching peak, typically found between  $1600-1650\text{ cm}^{-1}$ , which suggests the presence of carbonyl groups. Additionally, the O-H bending peak around  $1400-1450\text{ cm}^{-1}$  corresponds to the bending vibrations of hydroxyl groups, while the C-O stretching peak, typically observed in the range of  $1000-1200\text{ cm}^{-1}$ , represents the stretching vibrations of C-

O bonds in ether linkages within the starch molecule. The C-H bending peak, appearing around  $1300\text{-}1450\text{ cm}^{-1}$ , indicates the bending vibrations of C-H bonds in alkyl groups. Lastly, peaks around  $1020\text{-}1040\text{ cm}^{-1}$  and  $995\text{-}1015\text{ cm}^{-1}$  are indicative of the presence of amylose and amylopectin, respectively, within the rice and *Ulva* starch sample (Berkkan et al., 2021; Vaitkeviciene et al., 2022).

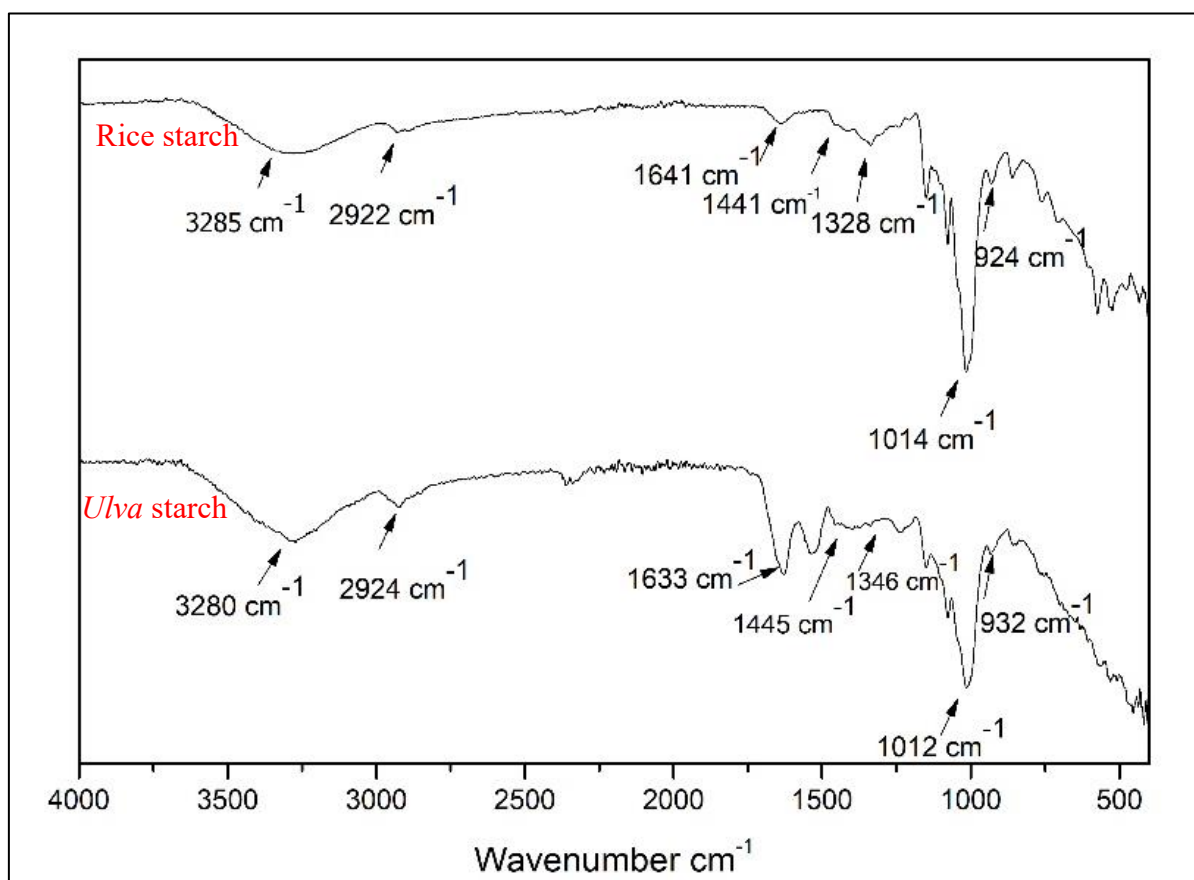


**Fig. 13:** FTIR graph of Rice and *Ulva* starch

Similar trend was seen in FTIR graph of rice and *Ulva* starch nanoparticles but with some minor variations like stretching and sharpness of hydroxyl and carbonyl peaks (**Fig. 14**).

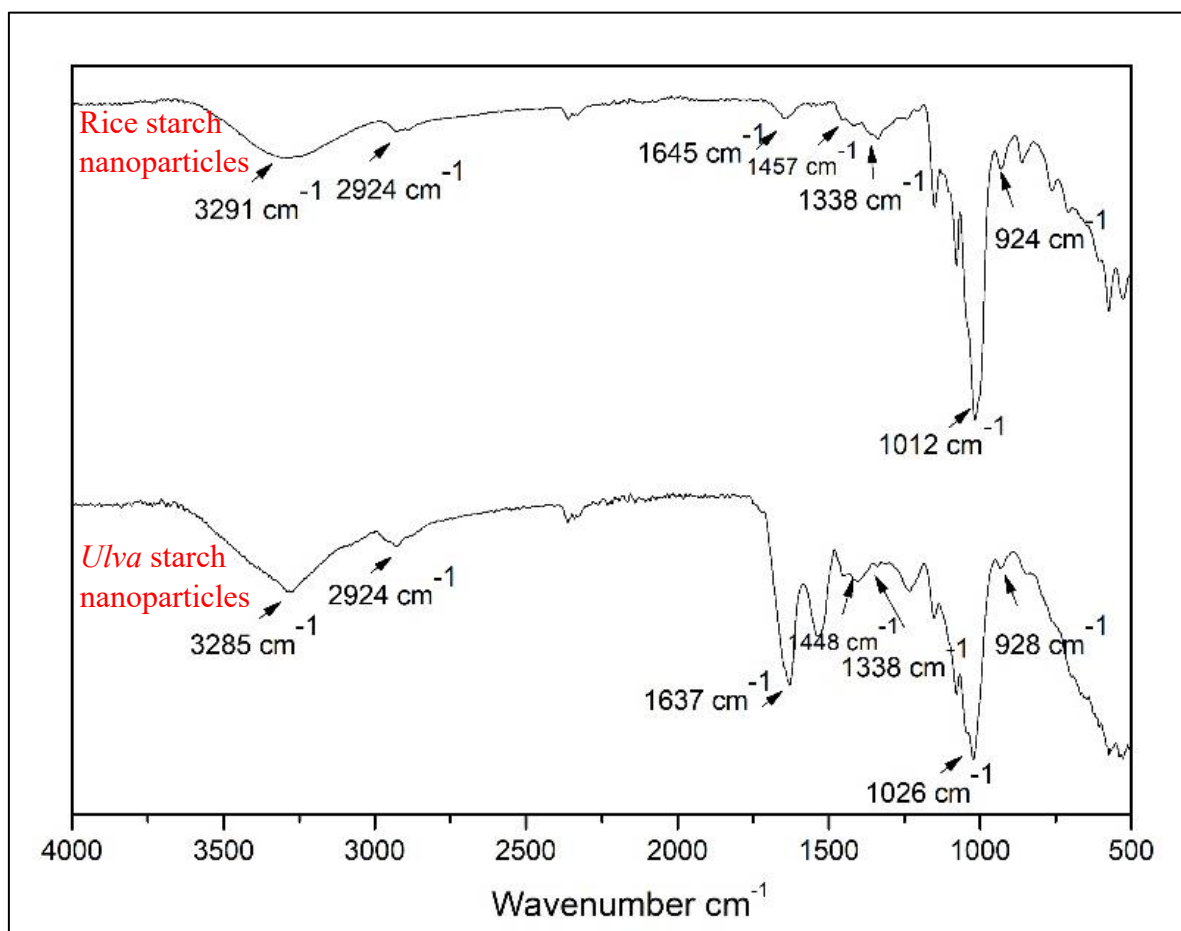


**Fig. 14:** FTIR graph of Rice and *Ulva* starch nanoparticles

For starch samples and starch nanoparticle samples, following peaks were observed as shown in the **Table No. 3**.

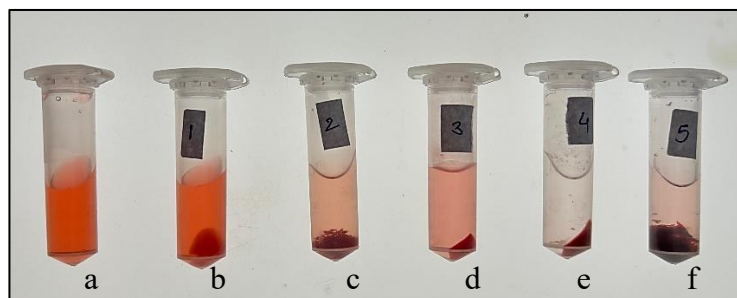
**Table No. 3:** Comparison of FTIR graph functional groups peaks theoretical (Berkkan et al., 2021; Vaitkeviciene et al., 2022) and observed.

Sr. No.	Type of functional group	Theoretical absorbance range (cm <sup>-1</sup> )	Absorbance (cm <sup>-1</sup> )			
			Rice starch	<i>Ulva</i> starch	Rice starch nanoparticles	<i>Ulva</i> starch nanoparticles
1	Hydroxyl group stretching (O-H)	3200-3600	3285	3280	3291	3285
2	Alkyl group stretching (C-H)	2900-2950	2922	2924	2924	2924
3	Carbonyl group stretching (C=O)	1600-1650	1641	1633	1645	1637
4	Hydroxyl group bending vibration (O-H)	1400-1450	1441	1445	1457	1448
5	Ether linkage (C-O)	1000-1200	1328	1346	1338	1338
6	Alkyl groups (C-H)	1300-1450	1014	1012	1012	1026
7	Amylose and amylopectin	1020-1040 and 995-1015	924	932	924	928

#### 4.4. Dye removal study

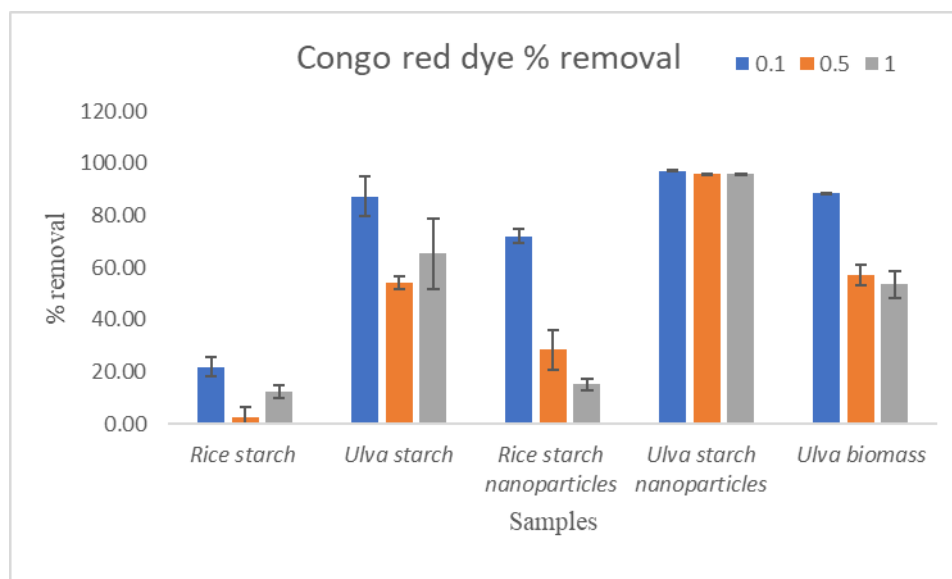
##### Congo red:

The image depicts the pelleted samples after the incubation period of 15 minutes with Congo red dye of concentration 0.1mg/mL (**Fig. 15**).



**Fig. 15:** Image showing various tubes of Congo red dye (0.1 mg/mL) removal by samples  
**a:** control, **b:** rice starch, **c:** *Ulva* starch, **d:** rice starch nanoparticles, **e:** *Ulva* starch nanoparticles, **f:** dry *Ulva* biomass

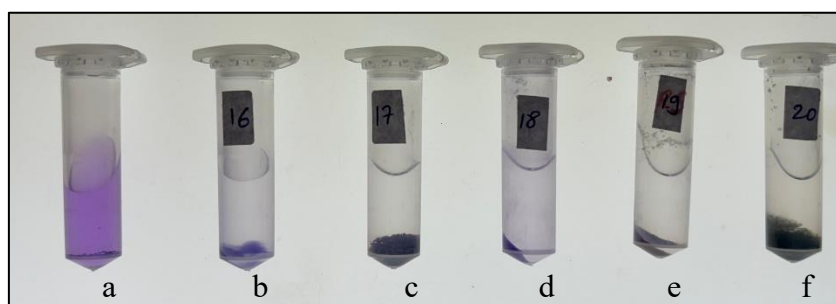
At all three concentrations (0.1 mg/mL, 0.5 mg/mL, 1 mg/mL) of Congo red, *Ulva* starch nanoparticles consistently demonstrated notably high and steady efficiency in dye removal, with percentages ranging from 95 % to 98 % (**Fig. 16**). However, both rice starch nanoparticles and *Ulva* biomass exhibited a significant decline in removal efficiency i.e., 72 % to 15 % and 88 % to 53 % respectively as the Congo red dye concentration increased from 0.1 mg/mL to 1 mg/mL. *Ulva* starch displayed varying removal percentage 87 %, 54 %, 65 % across 0.1 mg/mL, 0.5 mg/mL, 1 mg/mL concentrations tested. Among all the samples tested, rice starch exhibited the lowest removal percentage in range 21 % to 2 %.



**Fig. 16:** Image showing graphical representation of percent removal of Congo red dye (Concentration 0.1 mg/mL, 0.5 mg/mL, 1.0 mg/mL) by various samples.

### Crystal violet:

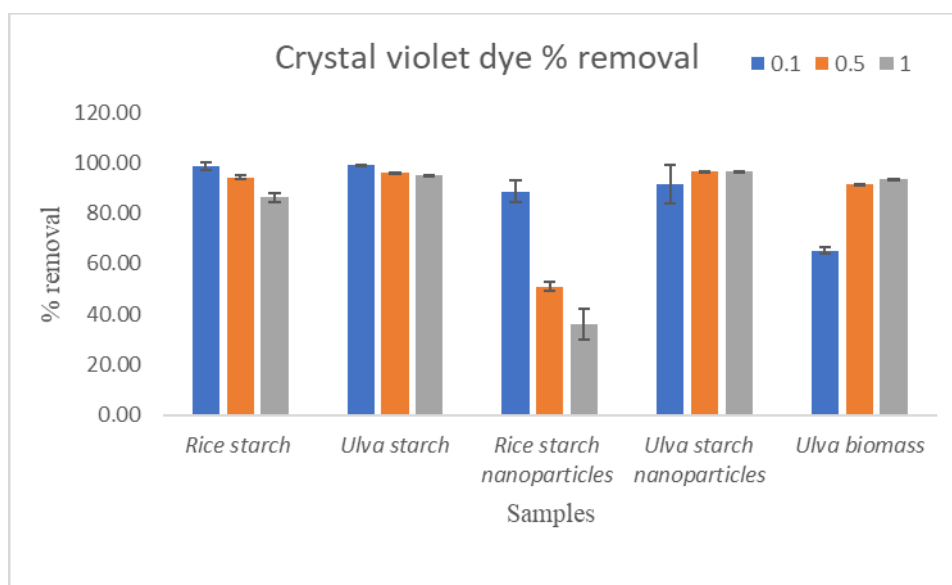
The image depicts the pelleted samples after the incubation period of 15 minutes with Crystal violet dye of concentration 0.1 mg/mL (**Fig. 17**).



**Fig. 17:** Image showing various tubes of Crystal violet dye (0.1 mg/mL) removal by samples **a:** control, **b:** rice starch, **c:** *Ulva* starch, **d:** rice starch nanoparticles, **e:** *Ulva* starch nanoparticles, **f:** dry *Ulva* biomass

*Ulva* starch, *Ulva* starch nanoparticles, and rice starch consistently exhibited the highest and stable efficiency in crystal violet removal, with percentages ranging from 98 % to 94 %, 91 % to 96 % and 98 % to 86 % respectively for all three concentrations (**Fig. 18**). However,

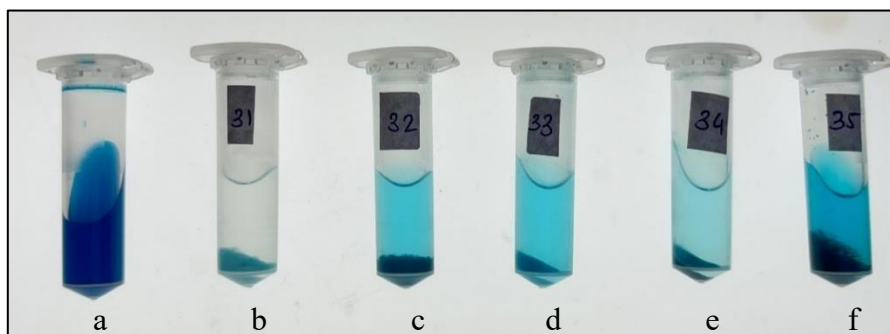
there was a decline in removal efficiency observed with increasing concentration of dye for rice starch nanoparticles. Additionally, *Ulva* biomass demonstrated high removal efficiency with the concentrations of 0.5 mg/mL and 1mg/mL, but its effectiveness was moderate for 0.1 mg/mL.



**Fig. 18:** Image showing graphical representation of percent removal of Crystal violet dye (Concentration 0.1 mg/mL, 0.5 mg/mL, 1.0 mg/mL) by various samples

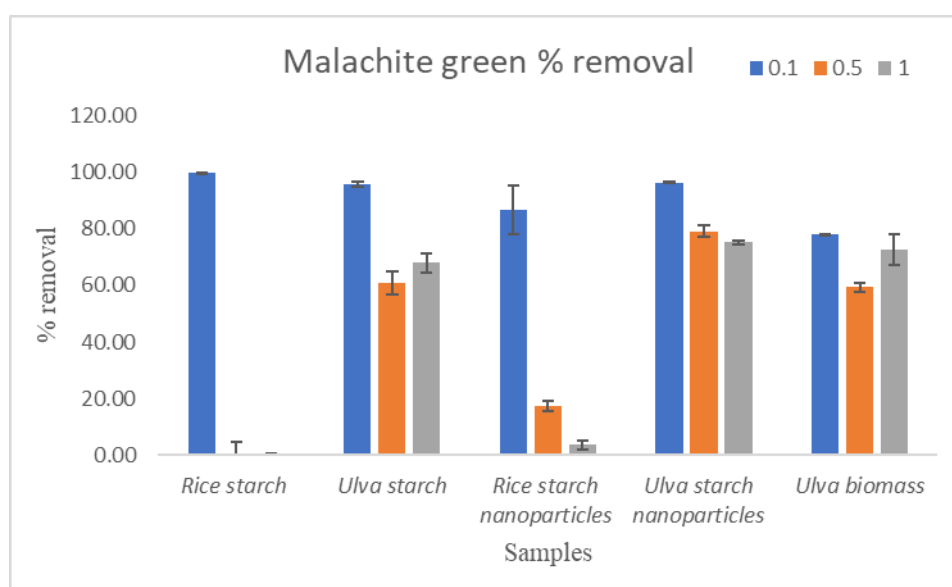
### Malachite green:

The image depicts the pelleted sample after the incubation period of 15 minutes with Malachite green dye of concentration 0.1 mg/mL (**Fig. 19**).



**Fig. 19:** Image showing various tubes of Malachite green dye (0.1 mg/mL) removal by samples **a:** control, **b:** rice starch, **c:** *Ulva* starch, **d:** rice starch nanoparticles, **e:** *Ulva* starch nanoparticles, **f:** dry *Ulva* biomass.

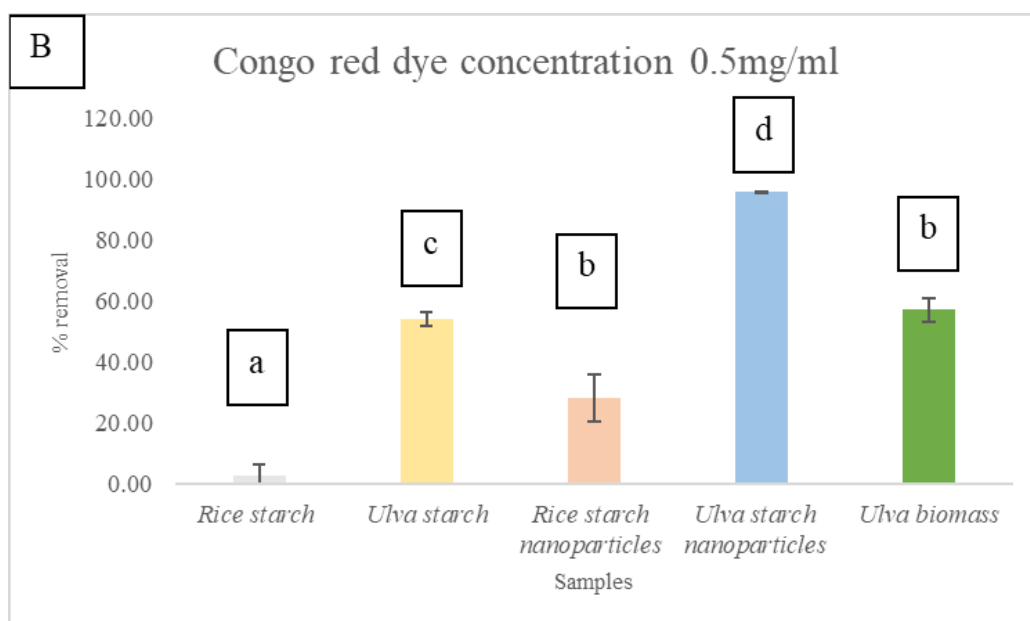
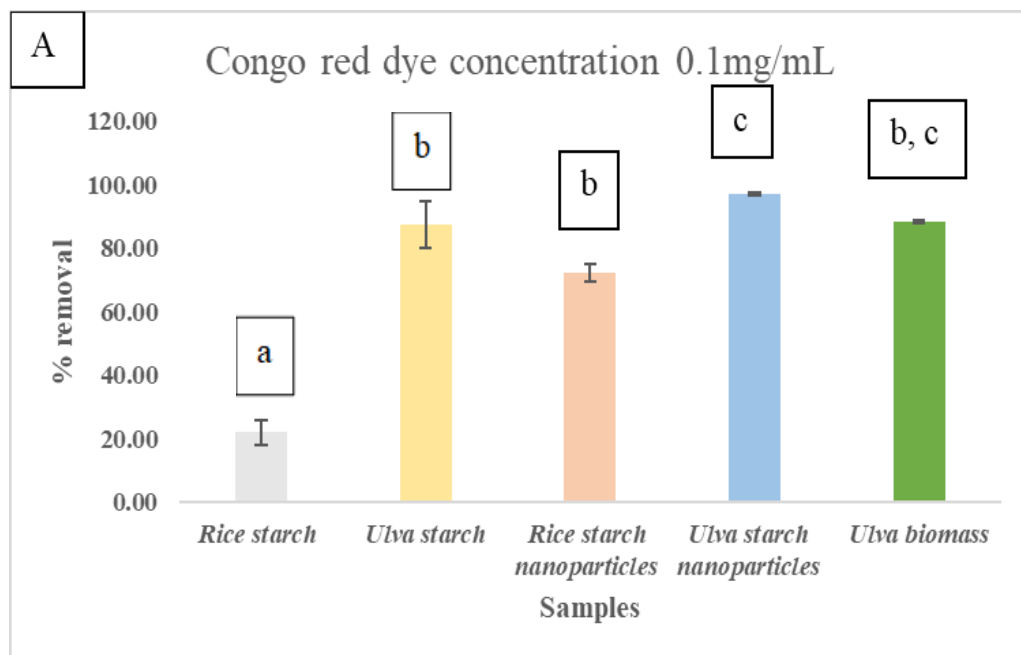
*Ulva* starch nanoparticles exhibited high dye removal efficiency for malachite green, but with a slight decrease as the concentration increased, ranging from 97 % to 75 %. *Ulva* starch displayed varying dye removal efficiency ranging from 95 % to 60 % and *Ulva* biomass displayed moderate removal efficiency ranging from 77 % to 59 % (**Fig. 20**). Conversely, both rice starch and rice starch nanoparticles demonstrated high removal efficiency of 99 % and 86 % respectively at a concentration of 0.1 mg/mL but the lowest efficiency of 0 % and 17 % to 3 % respectively at both 0.5 and 1.0 mg/mL concentrations.



**Fig. 20:** Image showing graphical representation of percent removal of Malachite green dye (Concentration 0.1 mg/mL, 0.5 mg/mL, 1.0 mg/mL) by various samples

#### 4.5 Statistical analysis of % dye removal using ANOVA

For Congo red dye:



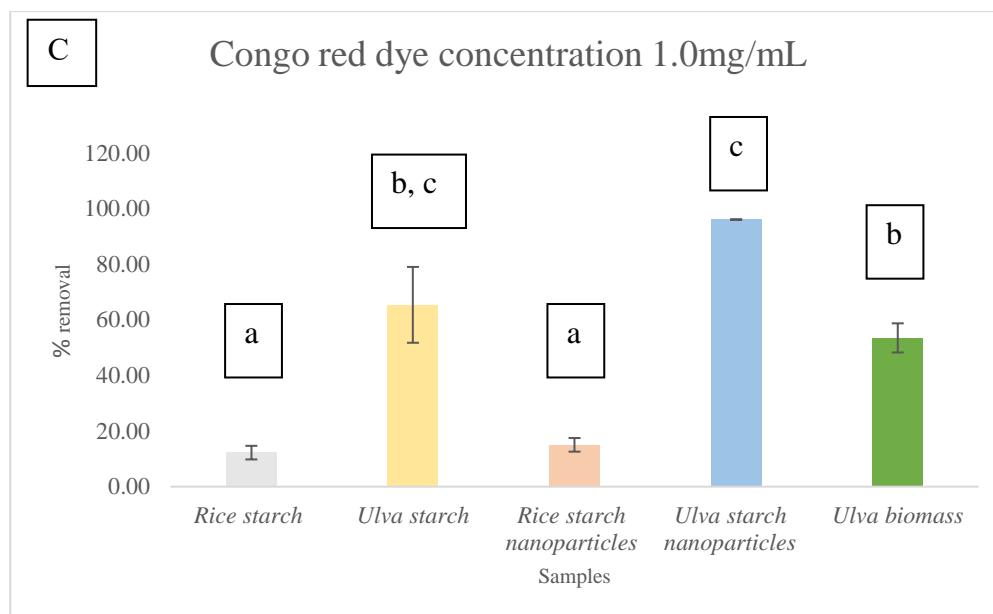
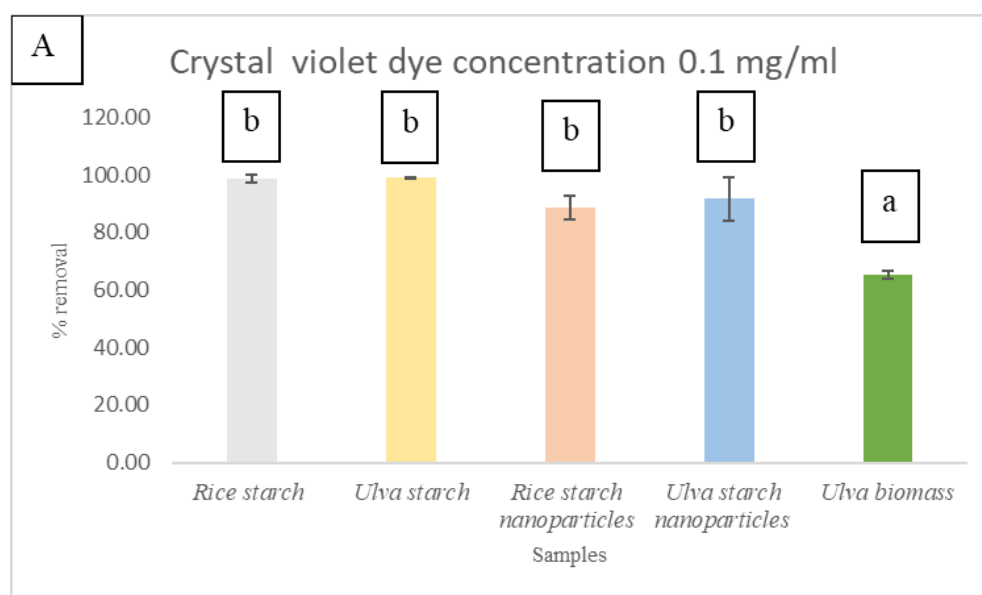


**Fig. 21:** Congo red dye concentration **A:** 0.1 mg/mL, **B:** 0.5 mg/mL, **C:** 1.0 mg/mL

The provided values represent the mean  $\pm$  standard deviation of two replicates ( $n = 2$ ) for each data point. In the bar graph, means marked with different superscript letters indicate statistically significant differences (determined through ANOVA with a significance level of  $p < 0.01$ , followed by post hoc multiple comparisons using Duncan's test).

In all three concentration 0.1, 0.5, 1.0 mg/mL of Congo red dye, *Ulva* starch nanoparticles showed significantly high percentage of dye removal having  $p < 0.001$  (Fig 21).

**For Crystal violet dye:**



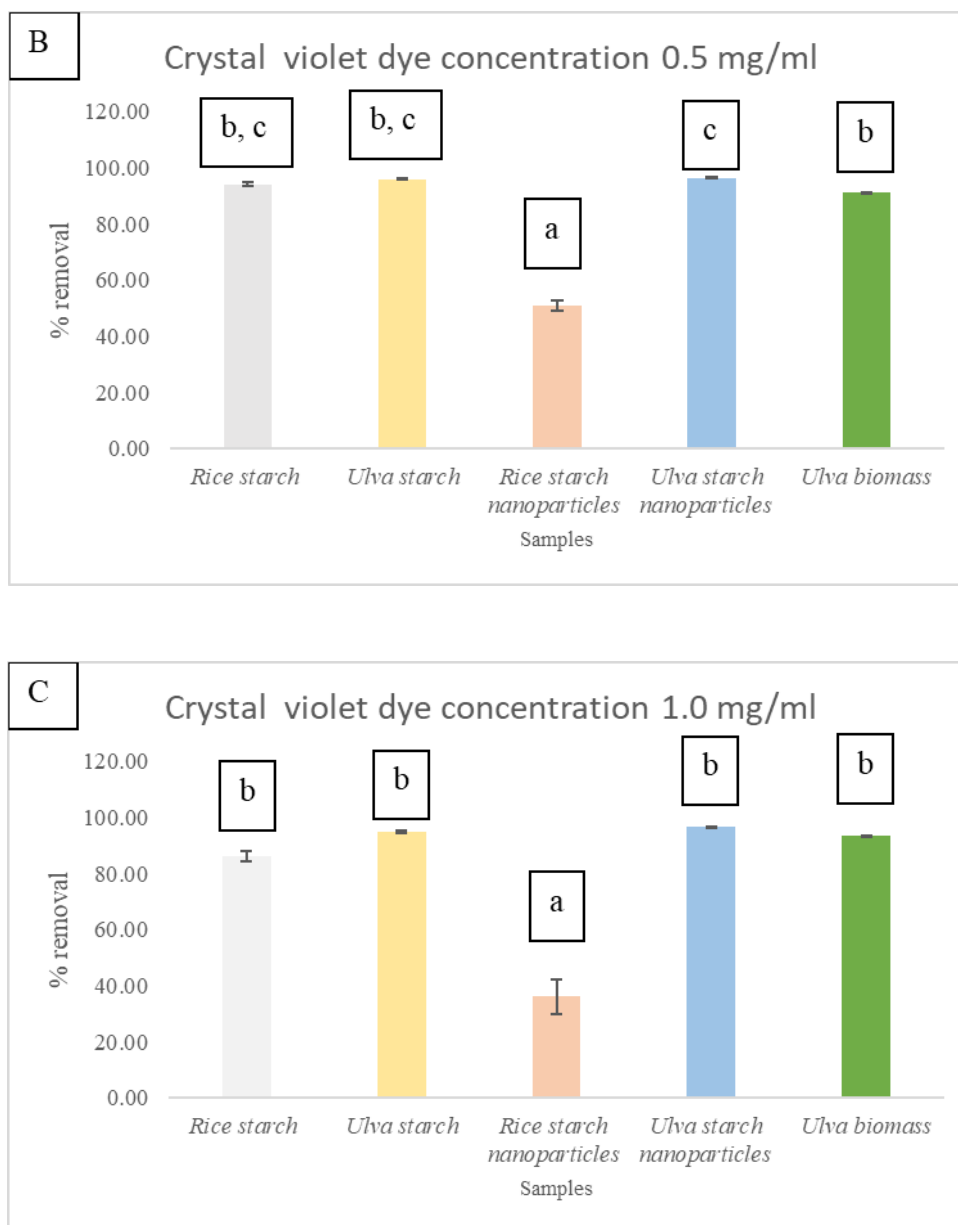


**Fig. 22:** Crystal violet dye concentration **A:** 0.1 mg/mL, **B:** 0.5 mg/mL, **C:** 1.0 mg/mL

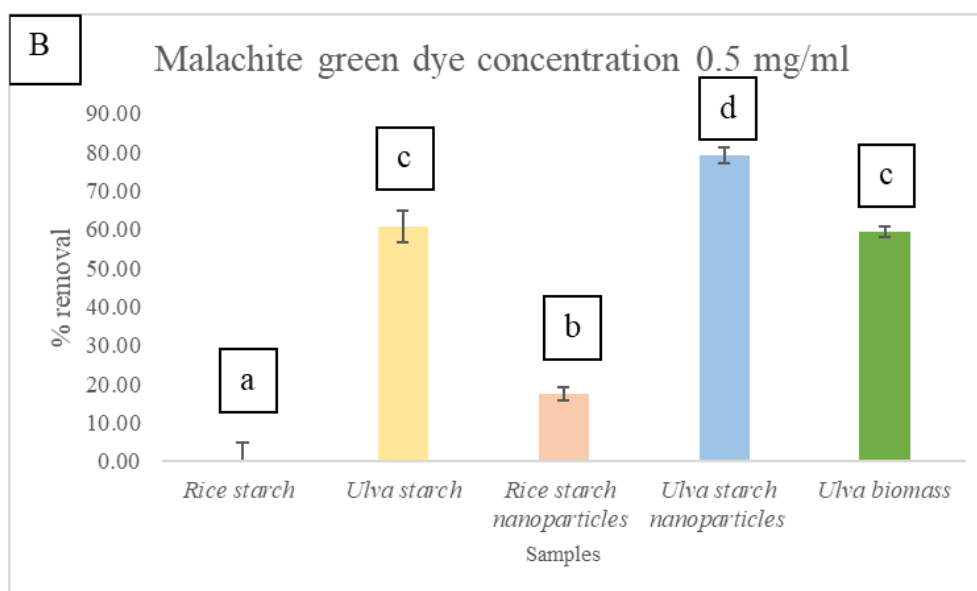
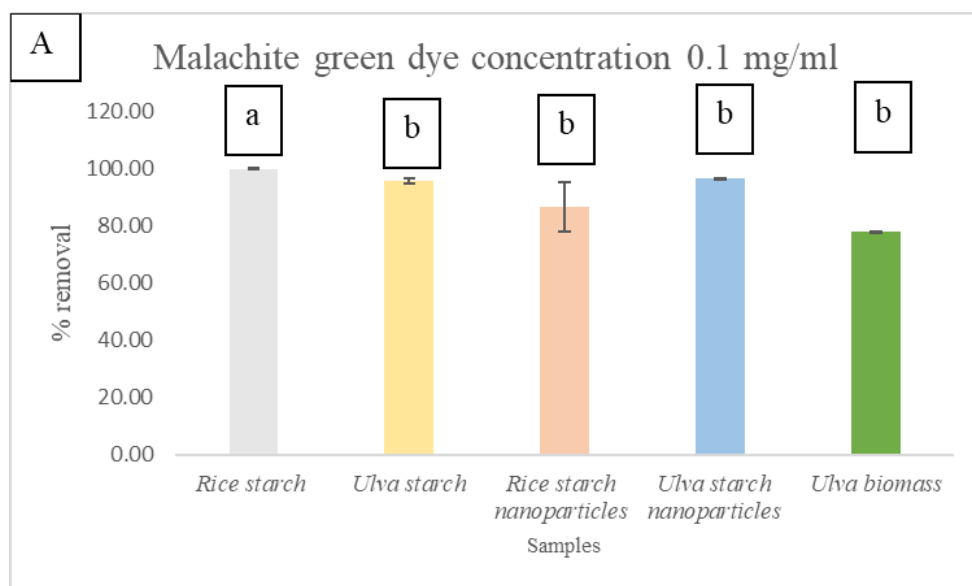
The provided values represent the mean  $\pm$  standard deviation of two replicates ( $n = 2$ ) for each data point. In the bar graph, means marked with different superscript letters indicate statistically significant differences (determined through ANOVA with a significance level of  $p < 0.01$ , followed by post hoc multiple comparisons using Duncan's test).

In concentration 0.1 mg/mL of Crystal violet dye, all samples expect for *Ulva* biomass sample showed significantly high percentage of dye removal having  $p=0.009$  (**Fig. 22 A**).

While in concentration 1.0 mg/mL all samples expect for rice starch nanoparticles sample

showed significantly ( $p=0.001$ ) high percentage of dye removal (**Fig. 22 C**). For 0.5 mg/mL concentration, *Ulva* starch nanoparticles along with *Ulva* starch and rice starch showed significantly ( $p=0.001$ ) high dye removal percentage (**Fig. 22 B**).

**For Malachite green dye:**



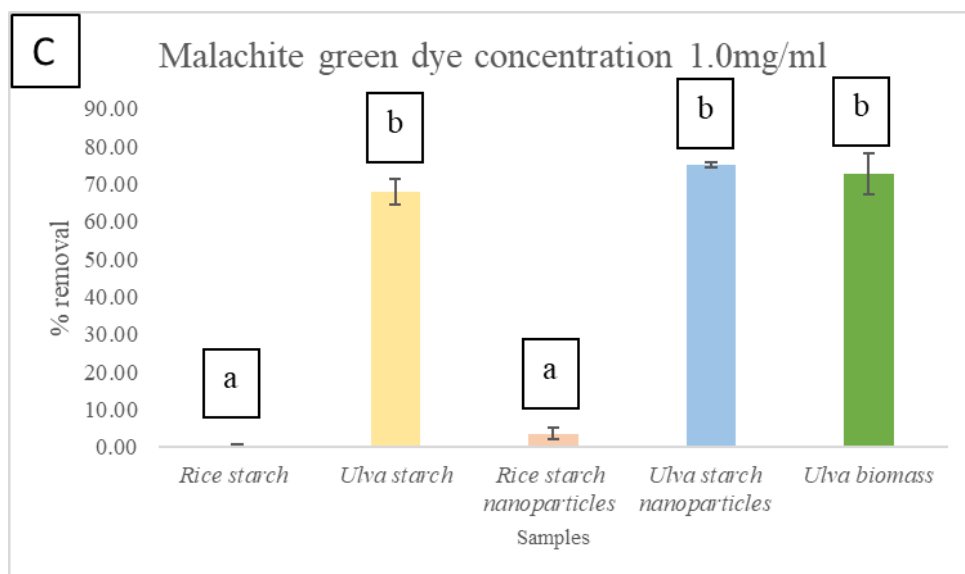


**Fig. 23:** Malachite green dye concentration **A:** 0.1 mg/mL, **B:** 0.5 mg/mL, **C:** 1.0 mg/mL

The provided values represent the mean  $\pm$  standard deviation of two replicates ( $n = 2$ ) for each data point. In the bar graph, means marked with different superscript letters indicate statistically significant differences (determined through ANOVA with a significance level of  $p < 0.01$ , followed by post hoc multiple comparisons using Duncan's test).

In concentration 0.1 mg/mL of Malachite green dye, % removal of all samples did not show any significance having  $p=0.048$  (**Fig. 23 A**). While in concentration 0.5 mg/mL *Ulva* starch nanoparticles showed significantly ( $p=0.001$ ) high percentage of dye removal (**Fig. 22 B**). For 1.0 mg/mL concentration, *Ulva* starch nanoparticles along with *Ulva* starch and *Ulva* biomass showed significantly ( $p=0.001$ ) high dye removal percentage (**Fig. 23 C**).

## **CONCLUSION**

In conclusion, the in-vitro cultivation of *Ulva* biomass revealed a growth rate of 4.45 % per day, indicating its potential as a sustainable resource. Characterization tests confirmed that the cultivated *Ulva* biomass retained its chemical composition, validating its successful cultivation. Furthermore, FTIR and SEM analyses demonstrated that *Ulva* starch and its nanoparticles exhibit similar characteristics to rice starch and its nanoparticles, respectively, suggesting their similarity to terrestrial starches and suitability for various applications. The results of the ANOVA analysis reveal significant differences among the experimental groups, indicating that there is a statistically significant effect of the independent variable (sample types: rice starch, rice starch nanoparticles, *Ulva* starch, *Ulva* starch nanoparticles, and *Ulva* biomass) on the dependent variable (percent removal of dyes: Congo red, Crystal violet, and Malachite green). This suggests that the sample type significantly influences the efficacy of dye removal. Particularly, *Ulva* starch and its nanoparticles exhibited promising capabilities for dye removal, even at higher concentrations, underscoring their potential as an effective and eco-friendly alternative for environmental remediation purposes. These findings highlight the potential of *Ulva* starch nanoparticles in the field of wastewater treatment particularly for dye removal.

## References

1. Lowry, O. H., Rosebrough, N. J., Farr, A. L., & Randall, R. J. (1951). Protein measurement with the Folin phenol reagent. *J Biol Chem*, 193(1), 265-275.
2. Shadangi, K. P., Sarangi, P. K., Behera, A. K. (Eds.). (2023). Chapter 3 - Characterization techniques of biomass: physico-chemical, elemental, and biological. In K. P. Shadangi, P. K. Sarangi, K. Mohanty, I. Deniz, & A. R. K. Gollakota (Eds.), *Bioenergy Engineering* (pp. 51-66).
3. Prabhu, M., Chemodanov, A., Gottlieb, R., Kazir, M., Nahor, O., Gozin, M., Israel, A., Livney, Y. D., & Golberg, A. (2019). Starch from the sea: The green macroalga *Ulva ohnoi* as a potential source for sustainable starch production in the marine biorefinery. *Algal Research*, 37(October 2018), 215–227.
4. Choi, H., Kim, W., & Shin, M. (2004). Properties of Korean Amaranth Starch Compared to Waxy Millet and Waxy Sorghum Starches. *Starch - Stärke*, 56(10), 469-477.
5. LUDWIG, T. G., & GOLDBERG, J. V. (1956). The anthrone method for the determination of carbohydrates in foods and in oral rinsing. *Journal of dental research*, 35(1), 90–94.
6. Dukare, A. S., Arputharaj, A., Bharimalla, A. K., Saxena, S., & Vigneshwaran, N. (2021). Nanostarch production by enzymatic hydrolysis of cereal and tuber starches. *Carbohydrate Polymer Technologies and Applications*, 2, 100121.
7. Boufi, S., Bel Haaj, S., Magnin, A., Pignon, F., Imp eror-Clerc, M., & Mortha, G. (2018). Ultrasonic assisted production of starch nanoparticles: Structural characterization and mechanism of disintegration. *Ultrasonics sonochemistry*, 41, 327–336.
8. Abid, N.; Khan, A.M.; Shujait, S.; Chaudhary, K.; Ikram, M.; Imran, M.; Haider, J.; Khan, M.; Khan, Q.; Maqbool, M. Synthesis of Nanomaterials Using Various Top-Down and Bottom-up Approaches, Influencing Factors, Advantages, and Disadvantages: A Review. *Adv. Colloid Interface Sci.* **2022**, 300, 102597.
9. Bayda, S., Adeel, M., Tuccinardi, T., Cordani, M., & Rizzolio, F. (2019). The History of Nanoscience and Nanotechnology: From Chemical-Physical Applications to Nanomedicine. *Molecules (Basel, Switzerland)*, 25(1), 112.
10. Chang, R., Ji, N., Li, M., Qiu, L., Sun, C., Bian, X., Qiu, H., Xiong, L., & Sun, Q. (2019). Green preparation and characterization of starch nanoparticles using a

- vacuum cold plasma process combined with ultrasonication treatment. *Ultrasonics Sonochemistry*, 58.
11. Chutia, H., & Mahanta, C. L. (2021). Properties of starch nanoparticle obtained by ultrasonication and high-pressure homogenization for developing carotenoids-enriched powder and Pickering nanoemulsion. *Innovative Food Science & Emerging Technologies*, 74.
  12. Cian, R. E., Drago, S. R., de Medina, F. S., & Martínez-Augustin, O. (2015). Proteins and Carbohydrates from Red Seaweeds: Evidence for Beneficial Effects on Gut Function and Microbiota. *Marine drugs*, 13(8), 5358–5383.
  13. Dai, L., Li, C., Zhang, J., & Cheng, F. (2018). Preparation and characterization of starch nanocrystals combining ball milling with acid hydrolysis. *Carbohydrate Polymers*, 180, 122-127.
  14. Gani, A., & Ashwar, B. A. (Eds.). (2021). Food biopolymers: Structural, functional and nutraceutical properties. doi:10.1007/978-3-030-27061-2
  15. Gul, K., Mir, N.A., Yousuf, B., Allai, F.M., Sharma, S. (2021). Starch: An Overview. In: Gani, A., Ashwar, B.A. (eds) Food biopolymers: Structural, functional and nutraceutical properties. Springer, Cham. [https://doi.org/10.1007/978-3-030-27061-2\\_1](https://doi.org/10.1007/978-3-030-27061-2_1)
  16. Guo, Z., Zhao, B., Chen, J., Chen, L., & Zheng, B. (2019). Insight into the characterization and digestion of lotus seed starch-tea polyphenol complexes prepared under high hydrostatic pressure. *Food Chemistry*, 297, 124992.
  17. Kim, J. H., Kim, J., Park, E. Y., & Kim, J. Y. (2017). Starch nanoparticles resulting from combination of dry heating under mildly acidic conditions and homogenization. *Carbohydrate polymers*, 168, 70–78.
  18. Liu, D., Wu, Q., Chen, H., & Chang, P. R. (2009). Transitional properties of starch colloid with particle size reduction from micro- to nanometer. *Journal of Colloid and Interface Science*, 339(1), 117-124.
  19. Marta, H., Rizki, D. I., Mardawati, E., Djali, M., Mohammad, M., & Cahyana, Y. (2023). Starch Nanoparticles: Preparation, Properties and Applications. *Polymers*, 15(5), 1167. <https://doi.org/10.3390/polym15051167>
  20. Marta, H., Rizki, D. I., Mardawati, E., Djali, M., Mohammad, M., & Cahyana, Y. (2023). Starch Nanoparticles: Preparation, Properties and Applications. *Polymers*, 15(5), 1167.
  21. National Geographic Society. (2021). Ocean.

22. Pan, X., Liu, P., Wang, Y., Yi, Y. -L., Zhang, H. -Q., Qian, D. -W., Xiao, P., Shang, E. -X., & Duan, J. -A. (2022). Synthesis of starch nanoparticles with controlled morphology and various adsorption rate for urea. *Food Chemistry*, 369.
23. PMF IAS. (2023). Coastline of India. Coastal Plains of India.
24. Prabhu, M., Chemodanov, A., Gottlieb, R., Kazir, M., Nahor, O., Gozin, M., Israel, A., Livney, Y. D., & Golberg, A. (2019). Starch from the sea: The green macroalga *Ulva ohnoi* as a potential source for sustainable starch production in the marine biorefinery. *Algal Research*, 37, 215-227.
25. UNESCO. (2023). Imminent risk of a global water crisis, warns the UN World Water Development Report 2023.
26. Union of International Associations (UIA). (2023). Declining agricultural land. World Problems & Global Issues. The Encyclopedia of World Problems. <https://uia.org/>
27. United Nations. (2019). World population projected to reach 9.8 billion in 2050, and 11.2 billion in 2100.
28. Wei, B., Cai, C., Xu, B., Jin, Z., & Tian, Y. (2018). Disruption and molecule degradation of waxy maize starch granules during high pressure homogenization process. *Food Chemistry*, 240, 165-173
29. Xiao, H., Yang, F., Lin, Q., Zhang, Q., Zhang, L., Sun, S., Han, W., & Liu, G. -Q. (2020). Preparation and characterization of broken-rice starch nanoparticles with different sizes. *International Journal of Biological Macromolecules*, 160, 437-445.
30. Xu, J., Liao, W., Liu, Y. et al. An overview on the nutritional and bioactive components of green seaweeds. *Food Prod Process and Nutr* 5, 18 (2023).
31. Yan, X., Diao, M., Yu, Y., Gao, F., Wang, E., Wang, Z., Zhang, T., & Zhao, P. (2022). Characterization of resistant starch nanoparticles prepared via debranching and nanoprecipitation. *Food Chemistry*, 369, 130824.
32. Yang, Y., Zhang, M., Alalawy, A. I., Almutairi, F. M., Al-Duais, M. A., Wang, J., & Salama, E.-S. (2021). Identification and characterization of marine seaweeds for biocompounds production. *Environmental Technology & Innovation*, 24, 101848. <https://doi.org/10.1016/j.eti.2021.101848>
33. Yu, S. K., Blennow, A., Bojko, M., Madsen, F., Olsen, C. E., & Engelsen, S. B. (2002). Physico-chemical characterization of floridean starch of red algae. *Starch-Starke*, 54(2), 66–74

34. Zollmann, M., Robin, A., Prabhu, M., Polikovskiy, M., Gillis, A., Greiserman, S., & Golberg, A. (2019). Green technology in green macroalgal biorefineries. *Phycologia*, 58(5), 516-534.
35. Durairaj, Sivakumar. (2014). Role of Lemna minor Lin. in Treating the Textile Industry Wastewater. 8. 55-59.
36. Abd El-Ghany, N. A., Elella, M. H. A., Abdallah, H. M., Mostafa, M. S., & Samy, M. (2023). Recent Advances in Various Starch Formulation for Wastewater Purification via Adsorption Technique: A Review. *Journal of Polymers and the Environment*, 31(7), 2792–2825.
37. Abrahart, E. N. (1977). *Dyes and their intermediates* (2nd ed). Edward Arnold.
38. Afkhami, A., & Moosavi, R. (2010). Adsorptive removal of Congo red, a carcinogenic textile dye, from aqueous solutions by maghemite nanoparticles. *Journal of Hazardous Materials*, 174(1–3), 398–403.
39. Ahamad, T., Naushad, Mu., Mousa, R. H., & Alshehri, S. M. (2020). Fabrication of starch-salicylaldehyde based polymer nanocomposite (PNC) for the removal of pollutants from contaminated water. *International Journal of Biological Macromolecules*, 165, 2731–2738.
40. Albuquerque, A. R. L., Angélica, R. S., Merino, A., & Paz, S. P. A. (2021). Chemical and mineralogical characterization and potential use of ash from Amazonian biomasses as an agricultural fertilizer and for soil amendment. *Journal of Cleaner Production*, 295, 126472.
41. Alderete, B. L., Da Silva, J., Godoi, R., Da Silva, F. R., Taffarel, S. R., Da Silva, L. P., Garcia, A. L. H., Júnior, H. M., De Amorim, H. L. N., & Picada, J. N. (2021). Evaluation of toxicity and mutagenicity of a synthetic effluent containing azo dye after Advanced Oxidation Process treatment. *Chemosphere*, 263, 128291.
42. Al-Tohamy, R., Ali, S. S., Li, F., Okasha, K. M., Mahmoud, Y. A.-G., Elsamahy, T., Jiao, H., Fu, Y., & Sun, J. (2022). A critical review on the treatment of dye-containing wastewater: Ecotoxicological and health concerns of textile dyes and possible remediation approaches for environmental safety. *Ecotoxicology and Environmental Safety*, 231, 113160.

43. Balina, K., Lika, A., Romagnoli, F., & Blumberga, D. (2017). Seaweed Cultivation Laboratory Testing: Effects of Nutrients on Growth Rate of *Ulva intestinalis*. *Energy Procedia*, 113, 454–459.
44. Berkkan, A., Kondolot Solak, E., & Asman, G. (2021). Starch-Based Membranes for Controlled Release of 5-Fluorouracil In Vitro. *ChemistrySelect*, 6(23), 5678–5684.
45. Bikker, P., Van Krimpen, M. M., Van Wikselaar, P., Houweling-Tan, B., Scaccia, N., Van Hal, J. W., Huijgen, W. J. J., Cone, J. W., & López-Contreras, A. M. (2016). Biorefinery of the green seaweed *Ulva lactuca* to produce animal feed, chemicals and biofuels. *Journal of Applied Phycology*, 28(6), 3511–3525.
46. Bligh, E. G., & Dyer, W. J. (1959). A RAPID METHOD OF TOTAL LIPID EXTRACTION AND PURIFICATION. *Canadian Journal of Biochemistry and Physiology*, 37(8), 911–917.
47. Braun, H. (1983). Particle Size and Solubility of Disperse Dyes. *Review of Progress in Coloration and Related Topics*, 13(1), 62–72.
48. Chatterjee, S., Lee, M. W., & Woo, S. H. (2010). Adsorption of congo red by chitosan hydrogel beads impregnated with carbon nanotubes. *Bioresource Technology*, 101(6), 1800–1806.
49. Cheng, R., Ou, S., Li, M., Li, Y., & Xiang, B. (2009). Ethylenediamine modified starch as biosorbent for acid dyes. *Journal of Hazardous Materials*, 172(2–3), 1665–1670.
50. Chinenye Adaobi Igwegbe. (2014). *Textile wastewater treatment using activated carbon from agro wastes*.
51. Dinesh Kumar, S., Satish, L., Dhanya, N., Malar Vizhi, J., Nadukkattu Nayagi, N., Gopala Krishnan, S., & Ganesan, M. (2023). Tank cultivation of edible seaweeds: An overview of the Indian perspective for opportunities and challenges. *Biomass Conversion and Biorefinery*.
52. Fang, X., Li, J., Li, X., Pan, S., Zhang, X., Sun, X., Shen, J., Han, W., & Wang, L. (2017). Internal pore decoration with polydopamine nanoparticle on polymeric ultrafiltration membrane for enhanced heavy metal removal. *Chemical Engineering Journal*, 314, 38–49.

53. Ganesamoorthy, R., Vadivel, V. K., Kumar, R., Kushwaha, O. S., & Mamane, H. (2021). Aerogels for water treatment: A review. *Journal of Cleaner Production*, 329, 129713.
54. Harris, G. K., & Marshall, M. R. (2017). Ash Analysis. In S. S. Nielsen (Ed.), *Food Analysis* (pp. 287–297). Springer International Publishing.
55. Hashimoto, T., Otori, M., Kashima, T., Yamamoto, H., & Tachibana, M. (2013). Chemical cystitis due to crystal violet dye: A case report. *Journal of Medical Case Reports*, 7(1), 145.
56. Ismail, H., Irani, M., & Ahmad, Z. (2013). Starch-Based Hydrogels: Present Status and Applications. *International Journal of Polymeric Materials*, 62(7), 411–420.
57. Khan, S., Zheng, H., Sun, Q., Liu, Y., Li, H., Ding, W., & Navarro, A. (2020). Synthesis and characterization of a novel cationic polyacrylamide-based flocculants to remove Congo red efficiently in acid aqueous environment. *Journal of Materials Science: Materials in Electronics*, 31(21), 18832–18843.
58. Khoo, P. S., Ilyas, R. A., Uda, M. N. A., Hassan, S. A., Nordin, A. H., Norfarhana, A. S., Ab Hamid, N. H., Rani, M. S. A., Abral, H., Norrahim, M. N. F., Knight, V. F., Lee, C. L., & Rafiqah, S. A. (2023). Starch-Based Polymer Materials as Advanced Adsorbents for Sustainable Water Treatment: Current Status, Challenges, and Future Perspectives. *Polymers*, 15(14), 3114.
59. Kidgell, J. T., Magnusson, M., De Nys, R., & Glasson, C. R. K. (2019). *Ulvan*: A systematic review of extraction, composition and function. *Algal Research*, 39, 101422.
60. Kim, J., Yoon, S., Choi, M., Min, K. J., Park, K. Y., Chon, K., & Bae, S. (2022). Metal ion recovery from electro dialysis-concentrated plating wastewater via pilot-scale sequential electrowinning/chemical precipitation. *Journal of Cleaner Production*, 330, 129879.
61. Kumari, H., Sonia, Suman, Ranga, R., Chahal, S., Devi, S., Sharma, S., Kumar, S., Kumar, P., Kumar, S., Kumar, A., & Parmar, R. (2023). A Review on Photocatalysis Used For Wastewater Treatment: Dye Degradation. *Water, Air, & Soil Pollution*, 234(6), 349.

62. Kumari, P., Kumar, M., Kumar, R., Kaushal, D., Chauhan, V., Thakur, S., Shandilya, P., & Sharma, P. P. (2024). Gum acacia based hydrogels and their composite for waste water treatment: A review. *International Journal of Biological Macromolecules*, 262, 129914.
63. Lawchoochaisakul, S., Monvisade, P., & Siriphannon, P. (2021). Cationic starch intercalated montmorillonite nanocomposites as natural based adsorbent for dye removal. *Carbohydrate Polymers*, 253, 117230.
64. Lellis, B., Fávoro-Polonio, C. Z., Pamphile, J. A., & Polonio, J. C. (2019). Effects of textile dyes on health and the environment and bioremediation potential of living organisms. *Biotechnology Research and Innovation*, 3(2), 275–290.
65. Li, C., Tang, T., Du, Y., Jiang, L., Yao, Z., Ning, L., & Zhu, B. (2023). *Ulvan* and *Ulva* oligosaccharides: A systematic review of structure, preparation, biological activities and applications. *Bioresources and Bioprocessing*, 10(1), 66.
66. Lin, J., Ye, W., Xie, M., Seo, D. H., Luo, J., Wan, Y., & Van Der Bruggen, B. (2023). Environmental impacts and remediation of dye-containing wastewater. *Nature Reviews Earth & Environment*, 4(11), 785–803.
67. Mani, S., & Bharagava, R. N. (2016). Exposure to Crystal Violet, Its Toxic, Genotoxic and Carcinogenic Effects on Environment and Its Degradation and Detoxification for Environmental Safety. In W. P. De Voogt (Ed.), *Reviews of Environmental Contamination and Toxicology Volume 237* (Vol. 237, pp. 71–104). Springer International Publishing.
68. Mona, S., Kaushik, A., & Kaushik, C. P. (2011). Waste biomass of *Nostoc linckia* as adsorbent of crystal violet dye: Optimization based on statistical model. *International Biodeterioration & Biodegradation*, 65(3), 513–521.
69. Moyo, S., Makhanya, B. P., & Zwane, P. E. (2022). Use of bacterial isolates in the treatment of textile dye wastewater: A review. *Heliyon*, 8(6), e09632.
70. Nguyen, T. P. T., Nguyen, D. V., Thuc, C. N. H., Bui, Q. B., Perré, P., & Nguyen, D. M. (2022). Valorization of starch nanoparticles on microstructural and physical properties of PLA -starch nanocomposites. *Journal of Applied Polymer Science*, 139(10), 51757.

71. Ortega-Toro, R., Santagata, G., Gomez d'Ayala, G., Cerruti, P., Talens Oliag, P., Chiralt Boix, M. A., & Malinconico, M. (2016). Enhancement of interfacial adhesion between starch and grafted poly( $\epsilon$ -caprolactone). *Carbohydrate Polymers*, *147*, 16–27.
72. Pappou, S., Dardavila, M. M., Savvidou, M. G., Louli, V., Magoulas, K., & Voutsas, E. (2022). Extraction of Bioactive Compounds from *Ulva lactuca*. *Applied Sciences*, *12*(4), 2117.
73. Peramune, D., Manatunga, D. C., Dassanayake, R. S., Premalal, V., Liyanage, R. N., Gunathilake, C., & Abidi, N. (2022). Recent advances in biopolymer-based advanced oxidation processes for dye removal applications: A review. *Environmental Research*, *215*, 114242.
74. Pezoa-Conte, R., Leyton, A., Baccini, A., Ravanal, M. C., Mäki-Arvela, P., Grénman, H., Xu, C., Willför, S., Lienqueo, M. E., & Mikkola, J.-P. (2017). Aqueous Extraction of the Sulfated Polysaccharide *Ulvans* from the Green Alga *Ulva rigida*—Kinetics and Modeling. *BioEnergy Research*, *10*(3), 915–928.
75. Prabhu, M., Chemodanov, A., Gottlieb, R., Kazir, M., Nahor, O., Gozin, M., Israel, A., Livney, Y. D., & Golberg, A. (2019). Starch from the sea: The green macroalga *Ulva ohnoi* as a potential source for sustainable starch production in the marine biorefinery. *Algal Research*, *37*, 215–227.
76. Putra, N. R., Fajriah, S., Qomariyah, L., Dewi, A. S., Rizkiyah, D. N., Irianto, I., Rusmin, D., Melati, M., Trisnawati, N. W., Darwati, I., & Arya, N. N. (2024). Exploring the potential of *Ulva Lactuca*: Emerging extraction methods, bioactive compounds, and health applications – A perspective review. *South African Journal of Chemical Engineering*, *47*, 233–245.
77. Rafiee, F. (2023). Alginate: Wastewater Treatment. In *Biochemistry* (Vol. 0). IntechOpen.
78. Ramos, A. H., Rockenbach, B. A., Ferreira, C. D., Gutkoski, L. C., & De Oliveira, M. (2019). Characteristics of Flour and Starch Isolated from Red Rice Subjected to Different Drying Conditions. *Starch - Stärke*, *71*(7–8), 1800257.

79. Research Center for Oceanography, Indonesian Institute of Sciences, Jl. Pasir Putih No. 1 Ancol Timur, Jakarta 14430, Indonesia, & Rasyid, A. (2017). Evaluation of Nutritional Composition of The Dried Seaweed *Ulva lactuca* from Pameungpeuk Waters, Indonesia. *Tropical Life Sciences Research*, 28(2), 119–125.
80. Saiyad, M., Shah, N., Joshipura, M., Dwivedi, A., & Pillai, S. (2023). Chitosan and its derivatives in wastewater treatment application. *Materials Today: Proceedings*, S2214785323050630.
81. Semeraro, P., Rizzi, V., Fini, P., Matera, S., Cosma, P., Franco, E., García, R., Ferrándiz, M., Núñez, E., Gabaldón, J. A., Fortea, I., Pérez, E., & Ferrándiz, M. (2015). Interaction between industrial textile dyes and cyclodextrins. *Dyes and Pigments*, 119, 84–94.
82. Sharma, J., Sharma, S., & Soni, V. (2023). Toxicity of malachite green on plants and its phytoremediation: A review. *Regional Studies in Marine Science*, 62, 102911.
83. Sharma, R., Nath, P. C., Mohanta, Y. K., Bhunia, B., Mishra, B., Sharma, M., Suri, S., Bhaswant, M., Nayak, P. K., & Sridhar, K. (2024). Recent advances in cellulose-based sustainable materials for wastewater treatment: An overview. *International Journal of Biological Macromolecules*, 256, 128517.
84. Teo, S. H., Ng, C. H., Islam, A., Abdulkareem-Alsultan, G., Joseph, C. G., Janaun, J., Taufiq-Yap, Y. H., Khandaker, S., Islam, G. J., Znad, H., & Awual, Md. R. (2022). Sustainable toxic dyes removal with advanced materials for clean water production: A comprehensive review. *Journal of Cleaner Production*, 332, 130039.
85. Tsubaki, S., Nishimura, H., Imai, T., Onda, A., & Hiraoka, M. (2020). Probing rapid carbon fixation in fast-growing seaweed *Ulva meridionalis* using stable isotope <sup>13</sup>C-labelling. *Scientific Reports*, 10(1), 20399.
86. Usman, M., Taj, M. B., & Carabineiro, S. A. C. (2023). Gum-based nanocomposites for the removal of metals and dyes from waste water. *Environmental Science and Pollution Research*, 30(46), 102027–102046.
87. Vaitkeviciene, R., Bendoraitiene, J., Degutyte, R., Svazas, M., & Zadeike, D. (2022). Optimization of the Sustainable Production of Resistant Starch in Rice Bran and

- Evaluation of Its Physicochemical and Technological Properties. *Polymers*, 14(17), 3662.
88. Verma, A., Thakur, S., Mamba, G., Prateek, Gupta, R. K., Thakur, P., & Thakur, V. K. (2020). Graphite modified sodium alginate hydrogel composite for efficient removal of malachite green dye. *International Journal of Biological Macromolecules*, 148, 1130–1139.
89. Vikrant, K., Giri, B. S., Raza, N., Roy, K., Kim, K.-H., Rai, B. N., & Singh, R. S. (2018). Recent advancements in bioremediation of dye: Current status and challenges. *Bioresource Technology*, 253, 355–367.
90. Vilpoux, O. F., & Santos Silveira Junior, J. F. (2023). Global production and use of starch. In *Starchy Crops Morphology, Extraction, Properties and Applications* (pp. 43–66). Elsevier.
91. Xiao, X., Chen, C., Deng, J., Wu, J., He, K., Xiang, Z., & Yang, Y. (2020). Analysis of trace malachite green, crystal violet, and their metabolites in zebrafish by surface-coated probe nanoelectrospray ionization mass spectrometry. *Talanta*, 217, 121064.
92. Yong, Y. S., Yong, W. T. L., & Anton, A. (2013). Analysis of formulae for determination of seaweed growth rate. *Journal of Applied Phycology*, 25(6), 1831–1834.
93. Zeng, L.-X., Chen, Y.-F., Zhang, Q.-Y., Kang, Y., & Luo, J.-W. (2014). Adsorption of congo red by cross-linked chitosan resins. *Desalination and Water Treatment*, 52(40–42), 7733–7742.
94. Zhao, S., Xia, Z., Liu, J., Sun, J., Zhang, J., & He, P. (2023). Morphology, growth, and photosynthesis of *Ulva prolifera* O.F. Müller (Chlorophyta, Ulvophyceae) gametophytes, the dominant green tide species in the Southern Yellow Sea. *Journal of Sea Research*, 193, 102375.

## Appendix

### 1. Instruments used:

- MRC Ultrasonic Processor, SONIC-650WT-V2
- UV-Vis spectrophotometer mini 1240
- Lab India Micro table high speed refrigerated centrifuge
- Redmi cis-24 plus incubator shaker
- Benchmark beadbug™ Mini Homogenizer Model D1030 (E)
- Thermo fisher medifuge small benchtop centrifuge
- Erma Head Refractometer
- Parthak electronic furnace

### 2. Reagents used for protein estimation by Folin's Lowry

Reagent A: 2% sodium carbonate in 0.1 N sodium hydroxide

Reagent B: 0.5% copper sulphate in 1% potassium sodium tartarate. Prepared freshly by mixing stock solution

Reagent C (Alkaline copper sulphate): Add 50mL of Reagent A and 1mL of Reagent B prior to use.

Folin's reagent (Reagent D): Dilute Folin-Ciocaltean with an equal volume of 0.1 N NaOH

Standard: 1mg/mL of BSA

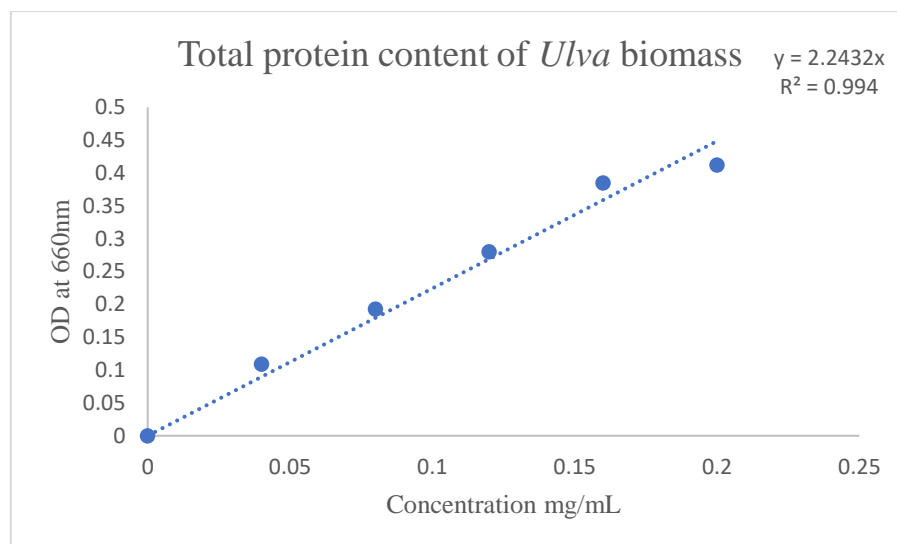


**Fig. 24:** Standard graph of total protein estimation in dry *Ulva* biomass

3. Reagents for Carbohydrate estimation:

Anthrone reagent: 0.2g of Anthrone powder in 100mL of concentrated  $H_2SO_4$ .

Freshly prepared reagent was used and stored in amber color bottle.

Standard: 1mg/mL Glucose

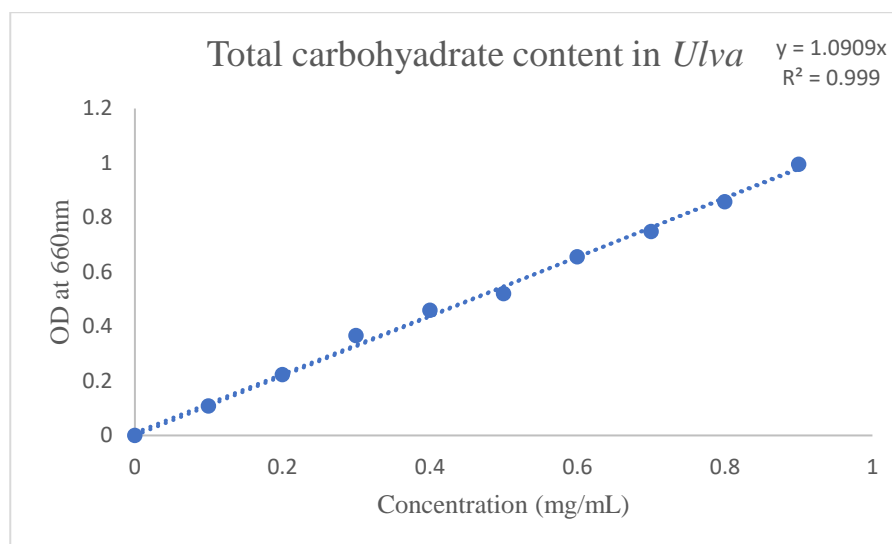


**Fig. 25:** Standard graph of total carbohydrate estimation in dry *Ulva* biomass